

The neocortex of cetartiodactyls: I. A comparative Golgi analysis of neuronal morphology in the bottlenose dolphin (*Tursiops truncatus*), the minke whale (*Balaenoptera acutorostrata*), and the humpback whale (*Megaptera novaeangliae*)

Camilla Butti · Caroline M. Janeway · Courtney Townshend ·
Bridget A. Wicinski · Joy S. Reidenberg · Sam H. Ridgway ·
Chet C. Sherwood · Patrick R. Hof · Bob Jacobs

Received: 14 May 2014 / Accepted: 25 July 2014
© Springer-Verlag Berlin Heidelberg 2014

Abstract The present study documents the morphology of neurons in several regions of the neocortex from the bottlenose dolphin (*Tursiops truncatus*), the North Atlantic minke whale (*Balaenoptera acutorostrata*), and the humpback whale (*Megaptera novaeangliae*). Golgi-stained neurons ($n = 210$) were analyzed in the frontal and temporal neocortex as well as in the primary visual and primary motor areas. Qualitatively, all three species exhibited a diversity of neuronal morphologies, with spiny neurons including typical pyramidal types, similar to those observed in primates and rodents, as well as other spiny neuron types that had more variable morphology and/or orientation. Five neuron types, with a vertical apical dendrite, approximated the general pyramidal neuron morphology (i.e., typical pyramidal, extraverted, magnopyramidal, multiapical, and bitufted

neurons), with a predominance of typical and extraverted pyramidal neurons. In what may represent a cetacean morphological apomorphy, both typical pyramidal and magnopyramidal neurons frequently exhibited a tri-tufted variant. In the humpback whale, there were also large, star-like neurons with no discernable apical dendrite. Aspiny bipolar and multipolar interneurons were morphologically consistent with those reported previously in other mammals. Quantitative analyses showed that neuronal size and dendritic extent increased in association with body size and brain mass (bottlenose dolphin < minke whale < humpback whale). The present data thus suggest that certain spiny neuron morphologies may be apomorphies in the neocortex of cetaceans as compared to other mammals and that neuronal dendritic extent covaries with brain and body size.

C. Butti (✉) · B. A. Wicinski · P. R. Hof
Fishberg Department of Neuroscience and Friedman Brain
Institute, Icahn School of Medicine at Mount Sinai, Box 1639,
One Gustave L. Levy Place, New York, NY 10029, USA
e-mail: butticamilla@gmail.com

C. M. Janeway · C. Townshend · B. Jacobs
Laboratory of Quantitative Neuromorphology, Psychology,
Colorado College, 14 E. Cache La Poudre, Colorado Springs,
CO 80903, USA

J. S. Reidenberg
Center for Anatomy and Functional Morphology, Icahn School
of Medicine at Mount Sinai, One Gustave L. Levy Place,
New York, NY 10029, USA

S. H. Ridgway
National Marine Mammal Foundation, 2240 Shelter Island
Drive, San Diego, CA 92106, USA

C. C. Sherwood
Department of Anthropology, The George Washington
University, 2110 G Street NW, Washington, DC 20052, USA

Keywords Cetacean neocortex · Neuronal morphology ·
Golgi method · Brain evolution

Introduction

In recent years, social, cognitive, and behavioral observations on cetaceans (Connor 2007; Garland et al. 2013; Herman and Tavolga 1980; Marino 2002; Marino et al. 2007) have led to increased interest in the structure of their brain (Butti and Hof 2010; Butti et al. 2009, 2011; Glezer et al. 1992, 1993, 1995, 1998; Glezer and Morgane 1990; Hof et al. 1992, 1995; Hof and Sherwood 2005; Hof and Van der Gucht 2007; Huggenberger 2008; Manger 2006, 2013; Manger et al. 2004; Marino 2002; Marino et al. 2002, 2003a, b, 2004a, b, 2007; Montie et al. 2007, 2008; Patzke et al. 2013). Cetaceans are distinguished among other mammals because of their adaptation to an entirely aquatic life, which differentiates them from their

closest phylogenetic relatives, the terrestrial artiodactyls (Nikaido et al. 2001). From a comparative perspective, it is of interest to examine the organization of the cetacean brain not only to appreciate the diversification of nervous system structure among mammals, but also to explore the neuroanatomical evolution of one prominent lineage of large-brained fully aquatic mammals to compare with other taxa such as primates. The current rapid Golgi study constitutes part of an ongoing project documenting neuronal morphology in the neocortex (Jacobs et al. 2011, 2014a) in large-brained mammals not previously examined, thereby contributing to a limited database of comparative neuroanatomy (Manger et al. 2008). We examined neuronal morphology in neocortical samples from the bottlenose dolphin (*Tursiops truncatus*), the North Atlantic minke whale (*Balaenoptera acutorostrata*), and the humpback whale (*Megaptera novaeangliae*).

Cetacean brain research has focused on general anatomy, cytoarchitecture, and chemoarchitecture. In terms of anatomy, postmortem magnetic resonance imaging of several cetacean species has revealed the spatial arrangements and proportions of many brain structures (Hanson et al. 2013; Marino et al. 2001a, b, c, 2002, 2003a, b, 2004a, b, 2007, 2008; Oelschläger et al. 2008). The cetacean cortex is especially thin (Morgane et al. 1980) and, at least in odontocetes, is more convoluted than in any other mammal studied to date (Elias and Schwartz 1969; Ridgway and Brownson 1984). Particularly, the gyrification of the cetacean cortex (measured as the Gyrencephalic Index, GI; see Manger et al. 2012 for details), unlike in other mammalian orders, is independent of brain mass and higher than that of other mammalian species with comparable brain masses (Manger et al. 2012). At the cytoarchitectural level, it has been shown that the entire cetacean neocortex is agranular, with lack of an internal granular layer, layer IV (Butti et al. 2011; Furutani 2008; Hof and Sherwood 2005; Hof and Van der Gucht 2007; Jacobs et al. 1971, 1979, 1982, 1984, 1988). The cetacean cortex is further characterized by a thick layer I, a dense layer II, a wide pyramidal layer III, a thin pyramidal layer V containing very large, clustered pyramidal neurons, and a multiform layer VI (Butti et al. 2011; Glezer and Morgane 1990; Hof et al. 2005; Hof and Sherwood 2005; Hof and Van der Gucht 2007; Morgane et al. 1988). Cellular clustering has also been noted in several cortical regions, including the insula and the frontal pole, as well as the occipital cortex of some mysticetes (Hof et al. 2005; Hof and Van der Gucht 2007; Manger et al. 1998). The pronounced cytoarchitectural parcellation and diversity documented in these studies challenge the classical view of the cetacean cortex as being homogenous and poorly differentiated (Kesarev 1971, 1975). Chemoarchitectural investigations of the distribution of the calcium-binding proteins (CaBPs) calbindin

(CB), parvalbumin (PV), and calretinin (CR) provided evidence that ~95 % of CaBPs colocalize with GABA in the cetacean visual cortex, which is similar to other mammals (Glezer et al. 1993). The neurochemical distribution of CB, PV, and CR in cetaceans differs considerably from that observed in rodents and primates (Hof et al. 1999). However, this distribution is comparable to hedgehogs, insectivorous bats, and the phylogenetically related artiodactyls (Gatesy 1997; Geisler and Uhen 2003; Gingerich et al. 2001; Gingerich and Uhen 1998; Glezer et al. 1993, 1998; Hof et al. 1999, 2000a; Milinkovitch et al. 1998; Nikaido et al. 1999, 2001; Shimamura et al. 1997, 1999; Thewissen et al. 2001, 2007).

Because of the challenges involved in obtaining cetacean brain specimens with a postmortem delay and a fixation time optimal for neuromorphological analysis, much less is known about the neuronal typology of the cetacean neocortex, with very little data available on mysticetes (Kraus and Pilleri 1969b, c). The few investigations of cortical neuromorphology in odontocetes have been restricted to qualitative Golgi analyses. Despite inconsistencies in the definition of neuronal morphologies (Ferrer and Perera 1988; Furutani 2008; Garey et al. 1985), such studies support the presence of many neuronal types in the cetacean neocortex. In the striped dolphin (*Stenella coeruleoalba*), for example, several cortical neuron types have been documented besides typical pyramidal neurons (Ferrer and Perera 1988), including giant multipolar, bitufted, horizontal, bipolar, spiny stellate, inverted pyramidal neurons, and extraverted pyramidal neurons, similar to those described in the neocortex of hedgehogs, bats, and opossums (Ferrer et al. 1986a; Lopez-Mascaraque et al. 1986; Sanides and Sanides 1972). In the bottlenose dolphin, documented neuronal types include, in addition to a wide variety of pyramidal neurons, several non-pyramidal neurons such as stellate, bipolar, multipolar, and spindle-shaped neurons (Garey et al. 1985).

A general conclusion from these studies is that the cetacean neocortex is characterized by a variety of neuronal types comparable to those found in most terrestrial mammals (de Lima et al. 1990; Garey et al. 1985; Jacobs et al. 2011, 2014a; Peters and Jones 1984). More specifically, these investigations reveal that spiny neurons are predominantly pyramidal neurons, with the majority having a morphology that resembles the “typical” pyramidal neurons of primates and rodents. Notably, however, there is considerable variability in the morphologies as well as orientations of some pyramidal neurons beyond what is usually observed in primates and rodents. Most of the typical pyramidal neurons reside in layers II–V (Ferrer and Perera 1988; Garey et al. 1985), with a positive relationship between soma depth and the overall size of the neurons (Glezer and Morgane 1990). Thus, magnopyramidal

neurons, which exhibit an extended array of apical bifurcations and a more modest basilar skirt, are found in deep layers III and V (Garey et al. 1985). Atypical pyramidal neurons include (1) extraverted neurons, which exhibit multiple, branching apical dendrites and diminished basilar skirts (Morgane et al. 1990), (2) inverted pyramidal neurons with descending apical dendrites and ascending basilar skirts, and (3) horizontal pyramidal neurons with laterally oriented apical dendrites (Ferrer and Perera 1988; Garey et al. 1985). Spiny multipolar neurons without clear apical dendrites have been defined as “Sternzellen” (star-like neurons) in the Northern sei whale, *Balaenoptera borealis* (Kraus and Pilleri 1969b). Non-pyramidal neurons are present in all cortical layers as spiny and aspiny bipolar and multipolar neurons (Ferrer and Perera 1988; Garey et al. 1985).

The aim of the present study was fourfold: (1) to verify and extend qualitative descriptions of neuronal morphology in the cetacean neocortex, particularly in the two mysticetes (e.g., minke whale and humpback whale) that have never been examined in terms of neuronal morphology; (2) to provide quantitative data on the dendritic characteristics of these neurons to supplement qualitative descriptions; (3) to examine potential regional variation in the distribution of neuronal morphologies across frontal, visual, motor, and anterior/posterior temporal cortices; and (4) to examine possible quantitative species differences for those neurons documented in sufficient number (e.g., typical pyramidal and extraverted pyramidal neurons). In particular, the present data on cetacean neuronal morphology provide the basis for subsequent comparisons to those obtained in another cetartiodactyl, the giraffe (*Giraffa camelopardalis*; Jacobs et al. 2014a).

Materials and methods

Specimens

Tissue was collected from three cetacean species: one odontocete (a 39-year-old male bottlenose dolphin, brain mass 1,385 g, autolysis time (AT) <2 h), and two mysticetes (a young female North Atlantic minke whale, brain mass 1,810 g, AT ~20 h; and a ~2-year-old male humpback whale, brain mass 3,603 g, AT = 8 h). The bottlenose dolphin brain was provided by the National Marine Mammal Foundation and, initially, was immersion-fixed in 10 % neutral buffered formalin for 3 months. The brain was split down the interhemispheric cleft and half the hemisphere was sectioned. The minke whale and the humpback whale were stranded along the coasts of New York State and samples were collected under National Marine Fisheries Service (NOAA Fisheries) permission to

Dr. Reidenberg. Prior to Golgi staining, all three brains had been immersion-fixed in 4 % paraformaldehyde in 0.1 M phosphate buffer for different time periods (bottlenose dolphin, 10 months; minke whale, 35 months; humpback whale tissue blocks, 1 month). The present research protocol was approved by the Colorado College Institutional Review Board (#011311-1).

Tissue selection

Cortical blocks (1-cm thick) were removed from the visual and anterior temporal cortices of the left hemisphere in the bottlenose dolphin, the visual and motor cortices of the left hemisphere in the minke whale, and the visual, anterior temporal, posterior temporal, and frontal cortices of the left hemisphere in the humpback whale (Fig. 1). The visual cortex was removed at the apex of the hemisphere from the dorsal-most portion of the lateral gyrus, defined by the entolateral and lateral sulci (Garey et al. 1989; Glezer and Morgane 1990; Hof and Van der Gucht 2007; Ladygina et al. 1978; Ladygina and Supin 1977; Morgane et al. 1988; Revishchin and Garey 1989; Sokolov et al. 1972). In the

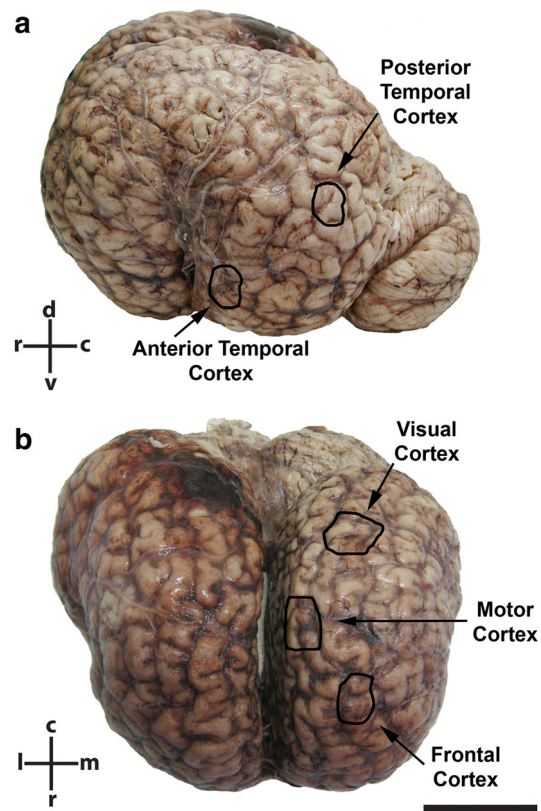


Fig. 1 Macroscopic view of the humpback whale brain. **a** Lateral view of left hemisphere indicating the sampling location of anterior and posterior temporal blocks. **b** Rostral view indicating the sampling location of visual, motor, and frontal blocks. Scale bar 5 cm

bottlenose dolphin and humpback whale, the anterior temporal cortex sample was removed from the ventroposterior aspect of the perisylvian gyrus, located posterior to the Sylvian fissure. In the minke whale, the motor cortex sample was removed from the domain extending from the anterior-most part of the lateral gyrus, located rostral to the visual field, to the cruciate sulcus (Glezer 2002; Kesarev and Malofeeva 1969). In the humpback whale, the posterior temporal cortex sample was removed from the posterolateral portion of the suprasylvian gyrus, defined by the lateral and suprasylvian sulci (Glezer 2002; Kesarev and Malofeeva 1969), and the frontal cortex sample was removed from the area that encompasses the polar gyri at the tip of the frontal lobe anteroventrally to the motor field. Although the whole brain was available for the three species, not all cortical regions were suitable for Golgi staining. Therefore, the selection of cortical regions was based on the best available tissue rather than prioritizing the comparison of the same cortical regions among species.

Tissue blocks were trimmed to a 3–5 mm thickness, coded to prevent experimenter bias, stained with a modified rapid Golgi technique (Scheibel and Scheibel 1978), and sectioned serially at 120 μm with a vibratome (Leica VT1000S, Leica Microsystems, Buffalo Grove, IL, USA). Tissue blocks adjacent to those removed for Golgi staining were examined with a routine Nissl stain to reveal cytoarchitecture.

Neuron selection and quantification

Neurons were selected for tracing based on established criteria (Anderson et al. 2009; Jacobs et al. 2011), which required an isolated soma near the center of the 120- μm section with fully impregnated, relatively unobscured, and complete dendritic arbors. Neurons were traced across all layers to encompass representative typologies and were quantified under a planachromatic 60 \times oil immersion objective along x -, y -, z -coordinates using the NeuroLucida software (MBF Bioscience, Inc., Williston, VT, USA), an Olympus BH-2 microscope equipped with a Ludl XY motorized stage (Ludl Electronics, Hawthorne, NY, USA), and a Heidenhain z -axis encoder (Schaumburg, IL, USA). A MicroFire Digital CCD 2-megapixel camera (Optronics, Goleta, CA, USA) mounted on a trinocular head (model 1-L0229, Olympus, Center Valley, PA, USA) displayed images on a 1,920 \times 1,200 resolution Dell E248WFP 24-inch LCD monitor. Somata were traced first at their widest point in the two-dimensional plane to provide an estimate of their cross-sectional area. Subsequently, dendrites were traced somatofugally in their entirety, recording dendritic diameter and number of spines, without differentiating the morphological types of spines. Dendritic arbors were not followed into adjacent sections, with

broken ends and ambiguous terminations identified as incomplete endings. A total of 210 neurons were traced by selecting all of those that met the inclusion criteria set out above. In the bottlenose dolphin ($n = 53$), 35 neurons were traced in visual and 18 in anterior temporal cortex. In the minke whale ($n = 60$), 39 neurons were traced in visual and 21 in motor cortex. In the humpback whale ($n = 97$), 28 neurons were traced in the visual cortex, 27 in frontal cortex, 26 in anterior temporal, and 16 in posterior temporal cortex.

The selected neurons were traced by two investigators (CJ and CT). Intra-rater reliability was determined by having each rater trace the same soma, dendritic segment, and spines ten times. The average coefficient of variation for soma size (3.1 %), total dendritic length (0.6 %), and dendritic spine number (3.8 %) indicated little variation in the tracings. Intra-rater reliability was further tested with a split plot design ($\alpha = 0.05$), which indicated no significant difference between the first five tracings and the last five tracings. Inter-rater reliability was determined by comparing ten dendritic system tracings with the same tracings completed by a senior investigator (BJ). Interclass correlations across soma size, total dendritic length, and dendritic spine number averaged 0.999, 0.998, and 0.996, respectively. An analysis of variance (ANOVA; $\alpha = 0.05$) indicated no significant difference among tracers for the three measures. Additionally, the primary investigator reexamined all completed tracings under the microscope to ensure accuracy.

Neuron descriptions and dependent dendritic and spine measurements

Qualitatively, neurons were classified according to somatodendritic criteria (Ferrer et al. 1986a, b; Jacobs et al. 2011) by considering factors such as soma size and shape, presence of spines, laminar location, and general morphology. Quantitatively, a centrifugal nomenclature was used to characterize branches extending from the soma as first-order segments, which bifurcate into second- and then third-order segments, and so on (Bok 1959; Uylings et al. 1986). In addition to quantifying soma size (using surface area, μm^2) and depth from the pial surface (μm), we examined six other measures that have been analyzed in previous studies (Jacobs et al. 2011): dendritic volume (Vol, μm^3 ; the total volume of all dendrites); total dendritic length (TDL, μm ; the summed length of all dendritic segments); mean segment length (MSL, μm ; the average length of each dendritic segment); dendritic segment count (DSC; the number of dendritic segments); dendritic spine number (DSN; the total number of spines on dendritic segments); and dendritic spine density (DSD; the average number of spines per μm of dendritic length). Additionally,

dendritic branching patterns were analyzed using a Sholl analysis (Sholl 1953), which quantified dendritic intersections at 20- μm intervals radiating somatofugally. Finally, the dendritic radius (distance from the soma to the distal end of the longest dendrite) of aspiny neurons was approximated on tracings to facilitate comparisons with findings in previous studies (Ferrer and Perera 1988; Hasiotis and Ashwell 2003; Jacobs et al. 2011; Kawaguchi 1995; Kisvarday et al. 1990; Lund and Lewis 1993; Meyer 1987; Peters and Regidor 1981; Somogyi et al. 1983). This last measure was obtained on all traced bipolar and multipolar neurons by the same investigator (CB) and the average of the measurements for each neuronal type across each species was taken as the final value, regardless of cortical region.

Independent variables and statistical analyses

Descriptive statistics obtained for the six dependent measures were aggregated for each neuron by species, neuron type, and cortical region. Because of the small sample size, inferential statistical analyses were limited to species differences in extraverted neurons and typical pyramidal neurons, which were the numerically dominant types of traced neurons. These neurons were evaluated on four

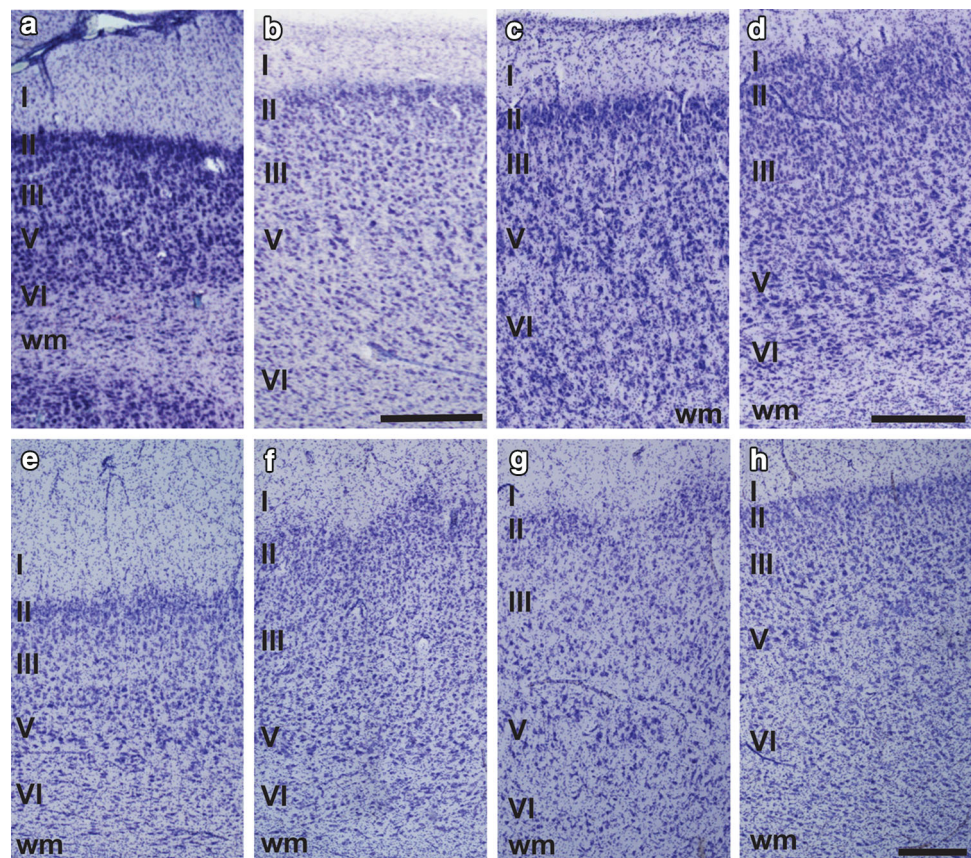
dependent variables: Vol, TDL, MSL, and DSC. DSN and DSD were not included because the quality of stained tissue varied among species, presumably due to differences in fixation times. An ANCOVA was used to identify significant differences across species. For these analyses, soma depth was partialled out as a covariate because there was a high Spearman's rho correlation between soma depth and the dependent measures for all traced neurons (Vol: $r_{(210)} = 0.65, p < 0.0001$; TDL: $r_{(210)} = 0.58, p < 0.0001$; MSL: $r_{(210)} = 0.51, p < 0.0001$; DSC: $r_{(210)} = 0.37, p < 0.0001$). In addition, for comparisons of apical dendrites (i.e., Sholl analyses), only neurons with relatively complete apical dendrites were included.

Results

Overview

Nissl stains in all species revealed a lack of layer IV, a relatively thick layer I, and a distinctly thin and cell-dense layer II (Fig. 2). The thickness of layers III, V, and VI varied across cortical regions among the three species. The humpback whale and minke whale cortices appeared thicker overall than that of the bottlenose dolphin. The

Fig. 2 Photomicrographs of Nissl-stained cortex from anterior temporal (a) and visual (b) cortices of the bottlenose dolphin; motor (c) and visual (d) cortices of the minke whale; anterior temporal (e), posterior temporal (f), frontal (g), and visual (h) cortices of the humpback whale. Layers are indicated in Roman numerals. Scale bar 400 μm



bottlenose dolphin, with the exception of the visual cortex, had more densely packed neurons in layers II, III, and V than did the humpback whale or the minke whale. Layer II was most distinct and cell-dense in the anterior temporal cortex of the bottlenose dolphin compared to the other regions and species. Neuron clustering was present in the posterior temporal and frontal cortices of the humpback whale, as previously reported by (Hof and Van der Gucht 2007). In general, neuronal density seemed to be higher in the bottlenose dolphin than in the two mysticetes, regardless of cortical region.

Golgi-stained tissue exhibited a higher quality impregnation for the humpback whale and the minke whale over the bottlenose dolphin and revealed a wide variety of neuronal sizes and morphologies (Figs. 3, 4, 5, 6). Quantitative data, broken down by species, cortical region, and neuron type are presented in Table 1. Soma size and dendritic extent were greater in the mysticetes compared to the bottlenose dolphin and highest in the humpback whale, as

confirmed by positive Spearman's rho correlations between brain mass and dependent measures for all traced neurons ($n = 210$; Vol: $r_{(210)} = 0.66$, $p < 0.0001$; TDL: $r_{(210)} = 0.57$, $p < 0.0001$; MSL: $r_{(210)} = 0.54$, $p < 0.0001$; DSC: $r_{(210)} = 0.30$, $p < 0.0001$; soma size: $r_{(210)} = 0.60$, $p < 0.0001$). In terms of morphology, the superficial layers II and III contained many small extra-verted pyramidal neurons with broad apical branching patterns, as well as some small typical pyramidal neurons with extensive basilar skirts. Layers V and VI contained neurons with larger somata, thicker apical dendrites, and more widely branching dendritic trees, as well as several atypical neuronal types.

Below, we discuss these neurons in more detail, with representative tracings depicted in Figs. 7, 8, 9, 10 for each species. Spiny neurons were classified as either pyramidal-like or nonpyramidal. Within the pyramidal-like designation, neurons were further divided by apical dendritic orientation and included typical pyramidal (i.e.,

Fig. 3 Photomicrographs of Golgi-impregnated neurons in visual (a–c) and anterior temporal (d–f) cortices of the bottlenose dolphin. Visual cortex: superficial typical and extraverted pyramidal neurons (a), extraverted pyramidal neurons (b), and aspiny multipolar neurons (c). Anterior temporal cortex: typical pyramidal neurons (d) and bitufted pyramidal neurons (e). High magnification of apical dendrites with relatively dense spines in the anterior temporal cortex (f). Scale bar 100 μm (a–e); 50 μm (f)

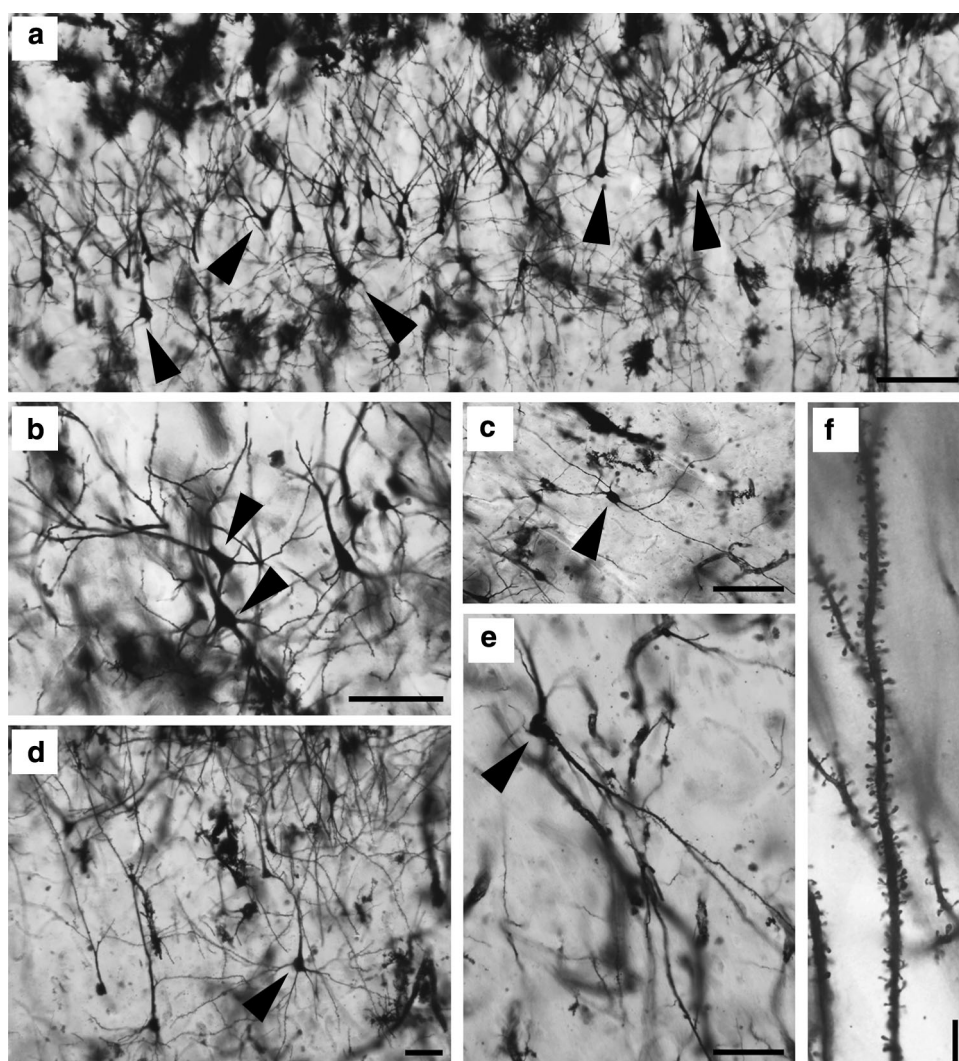
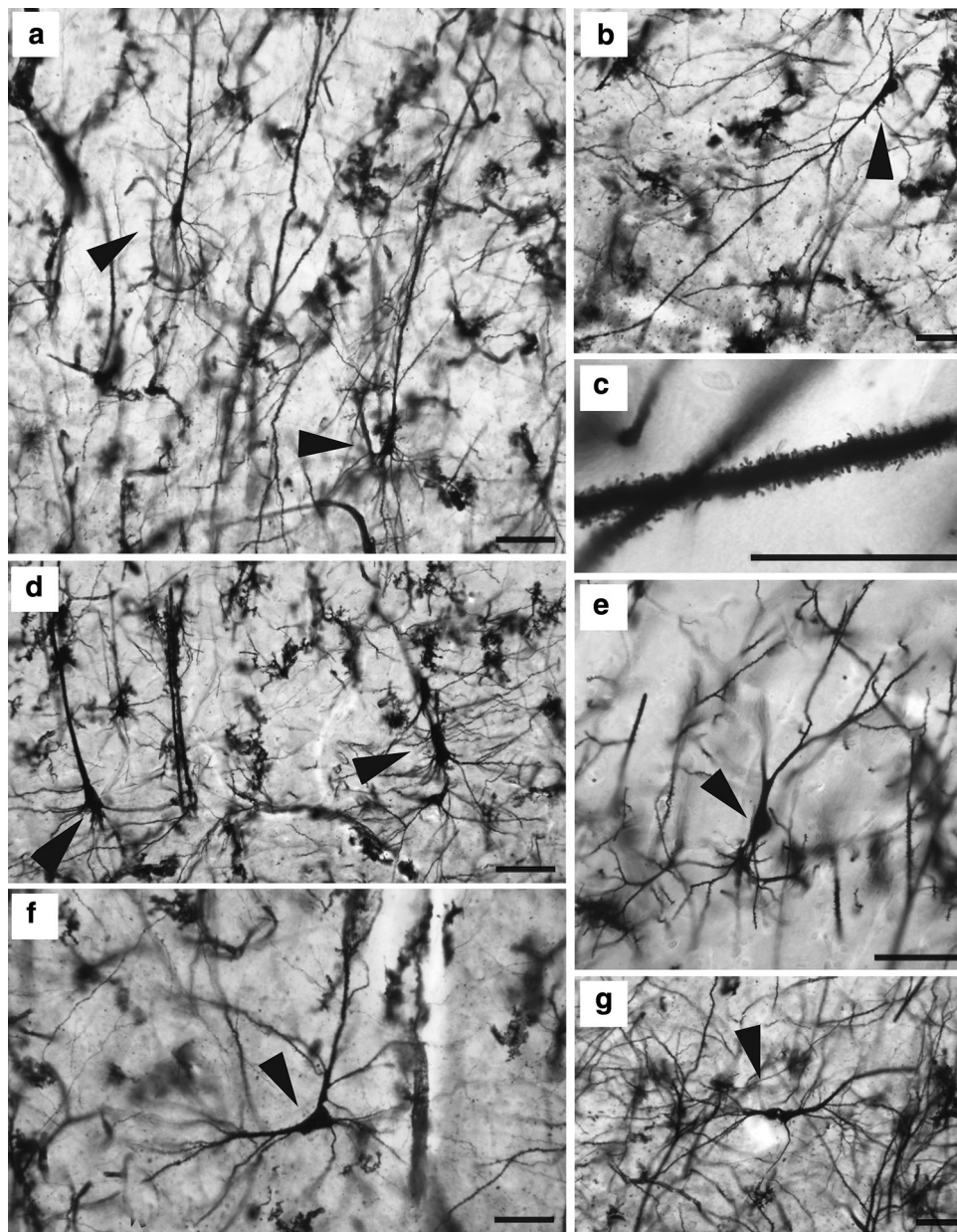


Fig. 4 Photomicrographs of Golgi-impregnated neurons in visual (a–c) and motor (d–g) cortices of the minke whale. Visual cortex: typical pyramidal neurons (a) and inverted pyramidal neurons (b). High magnification of dendrites with very dense dendritic spines (c). Motor cortex: magnopyramidal neurons (d), extraverted pyramidal neurons (e), horizontal pyramidal neurons (f), and flattened pyramidal neurons (g). Scale bar 100 μm (a, b, d–g); 50 μm (c)



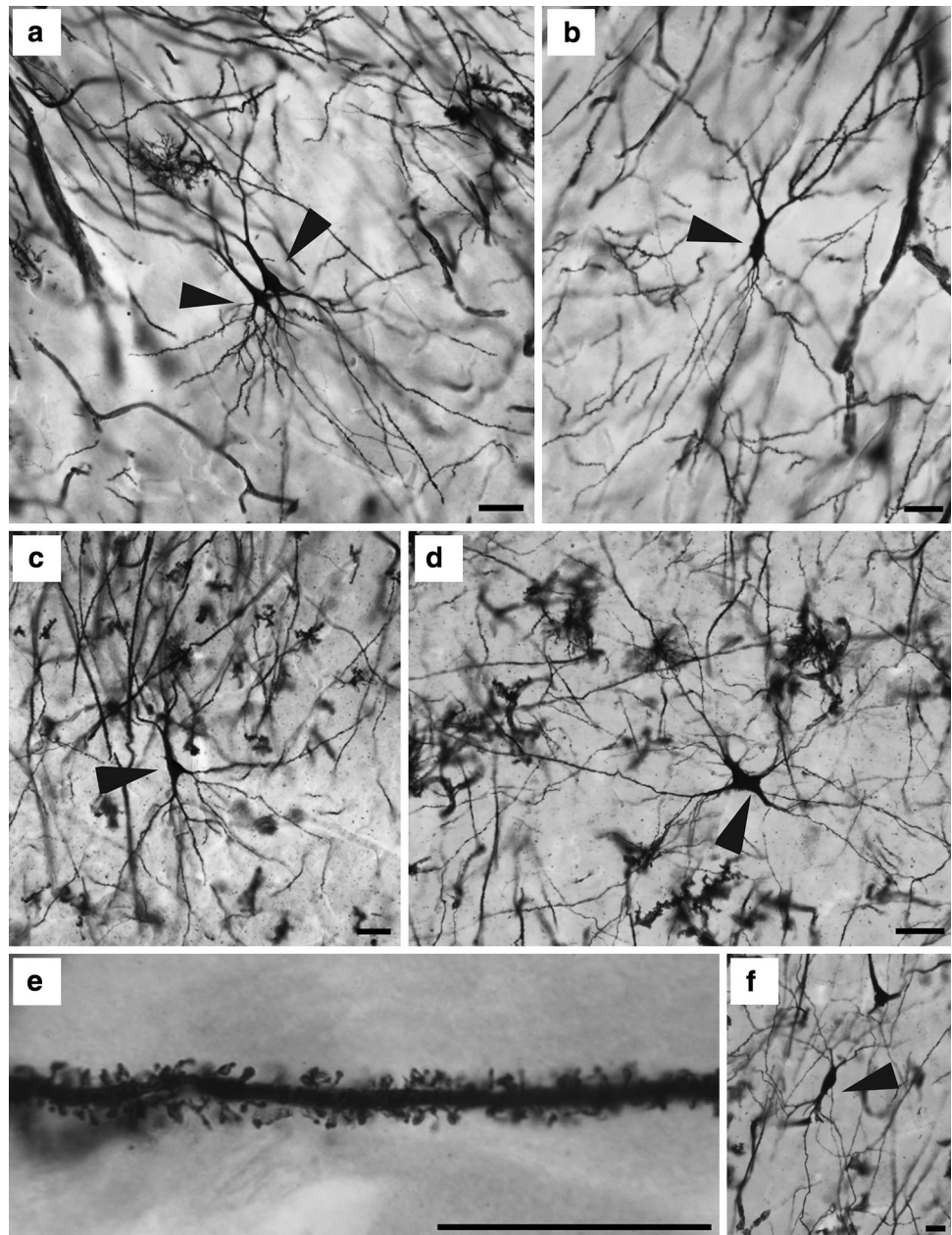
neurons resembling those in anthropoid primate and murid rodent species, with ascending, vertically oriented apical dendrites), extraverted pyramidal, magnopyramidal, multiapical pyramidal, and bitufted pyramidal neurons. Atypical pyramidal neurons (i.e., those that appeared unusual in orientation and/or morphology) included inverted pyramidal, horizontal pyramidal, and flattened pyramidal neurons. Nonpyramidal spiny neurons were classified as Sternzellen. Finally, aspiny neurons, which did not stain as prominently as spiny neurons, typically displayed either bipolar or multipolar morphologies. Sholl analyses for all neuron types are illustrated for spiny neurons in Fig. 11 and for aspiny neurons in Fig. 12.

Spiny neurons

Pyramidal-like neurons

Typical pyramidal neurons ($n = 80$; soma depth range 768–1,614 μm ; Table 1) were the most prevalent in the present study and were found across all cortical areas and in all species (Fig. 7a: D6–13; Fig. 7b: D18–26; Fig. 8a: M11–19; Fig. 8b: M31–39; Fig. 9a: H12–16; Fig. 9b: H27–29; Fig. 10a: H41–43; Fig. 10b: H55, H56). They possessed round, triangular, or oblong somata and were generally characterized by a single, ascending apical dendrite that branched as it neared the pial surface. Apical dendrite morphology varied, with some bifurcating into

Fig. 5 Photomicrograph of Golgi-impregnated neurons in anterior temporal (a, b, e) and posterior temporal (c, d, f) cortices of the humpback whale. Anterior temporal cortex: superficial typical pyramidal neurons (a) and extraverterted pyramidal neurons (b). High magnification of dendrite with very dense dendritic spines (e). Posterior temporal cortex: tri-tufted pyramidal neuron (c), Sternzellen (d), and aspiny bipolar neurons (f). Scale bar 100 μm (a–d, f); 50 μm (e)

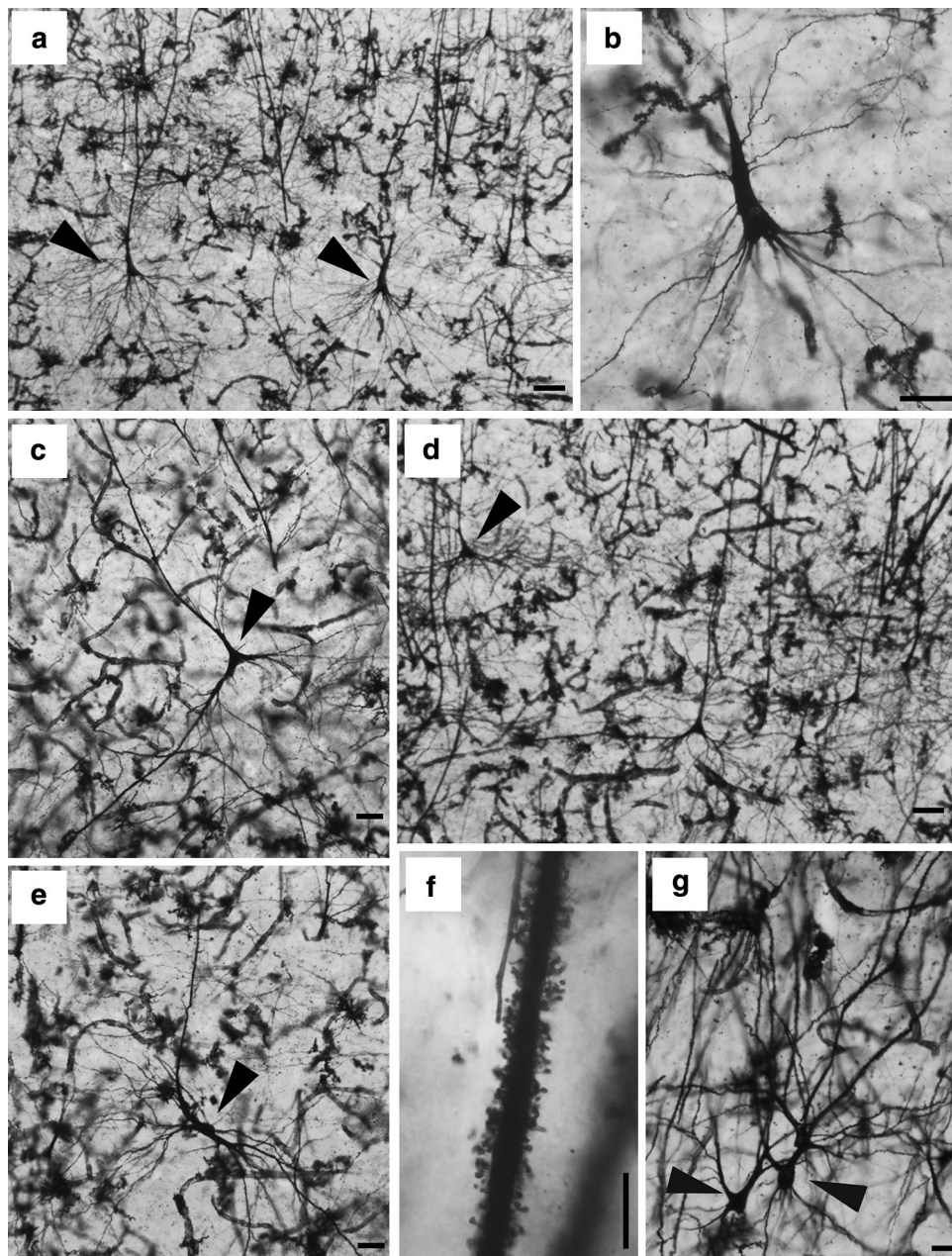


two, distinct branches close to the soma (Fig. 7b: D22, D24, D26; Fig. 8a: M12, M13; Fig. 8b: M35; Fig. 9a: H15; Fig. 9b: H27), and others continuing in a single shaft for a longer distance towards the pial surface before bifurcating into smaller branches (Fig. 7a: D11, D13; Fig. 8b: M36, M37; Fig. 10a: H42). Typical pyramidal neurons also possessed a well-developed basilar skirt (Figs. 3a, d, 4a, 5a, c), with an average of 4.85 ± 2.06 primary basilar dendrites that radiated in all directions. Several typical pyramidal neurons exhibited a tri-tufted appearance, with an ascending apical dendrite and two distinct basilar dendrites extending off the soma at roughly 90° to each other as lateral, and descending projections (Figs. 5c, 6c;

Fig. 7b: D23 and D25; Fig. 8a: M15, M16; Fig. 8b: M32; Fig. 10b: H56). Average DSD ranged from 0.17 to 0.75. In the Sholl analysis, basilar and apical dendritic density peaked near the soma, with basilar dendrites being denser than apical dendrites (Fig. 11). Basilar and apical dendritic distance from the soma was similar in the bottlenose dolphin and humpback whale, whereas apical dendrites were longer in the minke whale.

To ensure accurate comparisons for inferential statistics, only typical pyramidal neurons with relatively complete apical dendrites were analyzed (bottlenose dolphin, $n = 18$; minke whale, $n = 16$; humpback whale, $n = 14$). There were significant differences among all three species in

Fig. 6 Photomicrographs of Golgi-impregnated neurons in visual (a–f) and frontal (g) cortices of the humpback whale. Visual cortex: magnopyramidal neurons (a, b), tri-tufted magnopyramidal neurons (c, d) and flattened magnopyramidal neurons (e). High magnification of apical dendrite with very dense dendritic spines (f). Frontal cortex: extraverted pyramidal neurons (g). Scale bar 200 μm (a, d); 100 μm (b, c, e, g); 50 μm (f)



dendritic volume, increasing from bottlenose dolphin to minke whale (by 66.0 %) and from minke whale to humpback whale (by 62.5 %; $F_{(2,44)} = 27.46$, $p < 0.05$, $\eta_p^2 = 0.555$; Fig. 13). TDL in the humpback whale was significantly greater than that in both the minke whale (by 44.6 %) and the bottlenose dolphin (by 55.2 %; $F_{(2,44)} = 12.24$, $p < 0.05$, $\eta_p^2 = 0.357$). Both minke and humpback whales had significantly greater MSL values than did the bottlenose dolphin (by 28.0 and 34.6 %, respectively; $F_{(2,44)} = 9.30$, $p < 0.05$, $\eta_p^2 = 0.297$; Fig. 13). DSC was significantly greater in the humpback whale (by 40.7 %) and the bottlenose dolphin (by 22.0 %) than in the minke whale ($F_{(2,44)} = 9.21$, $p < 0.05$, $\eta_p^2 = 0.295$).

Extraverted pyramidal neurons ($n = 33$; soma depth range 476–1,297 μm ; Table 1) were found in layers II and superficial III in all cortical areas (Fig. 7a: D3; Fig. 7b: D16, D17; Fig. 8a: M1; Fig. 8b: M23, M24; Fig. 9a: H1, 2; Fig. 9b: H19–21; Fig. 10a: H33–35) except for the posterior temporal cortex of the humpback whale. These small- or medium-sized neurons possessed round or triangular somata, and were typified by an ascending apical shaft that bifurcated immediately upon leaving the soma (Figs. 3a, b, 4e, 5b, 6g). On average, dendritic extent was shorter in extraverted (TDL = 3,055 μm) than in typical pyramidal neurons (TDL = 3,881 μm). Further breakdown revealed that extraverted pyramidal neurons possess

Table 1 Summary statistics for cetacean neurons

Type	n^a	Vol. ^b	TDL ^c	MSL ^c	DSC ^d	DSN ^e	DSD ^f	SoSize ^g	SoDepth ^h
Spiny neurons									
<i>Bottlenose dolphin</i>									
Anterior temporal									
Bitufted	1	8,828	1,652	79	21	665	0.40	333	1,232
Extraverted	3	6,704 ± 1,409	2,315 ± 450	52 ± 7	48 ± 13	832 ± 91	0.38 ± 0.04	352 ± 50	949 ± 299
Multiapical	1	7,071	3,183	50	64	1,803	0.57	487	630
Typical	12	7,107 ± 474	3,159 ± 222	62 ± 5	53 ± 3	1,215 ± 183	0.38 ± 0.05	337 ± 26	890 ± 74
Visual									
Extraverted	5	5,183 ± 1,200	1,281 ± 185	52 ± 16	30 ± 5	94 ± 35	0.07 ± 0.02	307 ± 59	565 ± 131
Flattened	2	8,286 ± 1,316	2,308 ± 716	75 ± 3	31 ± 9	621 ± 273	0.26 ± 0.4	225 ± 21	864 ± 220
Magnopyramidal	1	17,680	4,381	61	72	713	0.16	574	1,084
Multiapical	1	18,107	4,062	77	53	1,231	0.30	519	860
Typical	23	9,215 ± 846	2,950 ± 209	53 ± 3	55 ± 2	534 ± 77	0.17 ± 0.02	372 ± 32	768 ± 64
<i>Minke whale</i>									
Motor									
Extraverted	2	7,863 ± 772	1,945 ± 752	71 ± 29	28 ± 1	1,306 ± 664	0.63 ± 0.10	335 ± 76	476 ± 120
Flattened	2	20,192 ± 3,804	3,536 ± 168	78 ± 8	46 ± 8	2,017 ± 3	0.57 ± 103	593 ± 119	1,090 ± 315
Horizontal	2	24,742 ± 779	4,690 ± 858	85 ± 10	55 ± 4	3,916 ± 1175	0.81 ± 0.10	850 ± 18	2,481 ± 1,032
Inverted	1	25,831	5,892	111	53	5,306	0.90	650	1,810
Magnopyramidal	5	40,562 ± 6,767	4,749 ± 503	80 ± 6	59 ± 3	3,426 ± 572	0.70 ± 0.05	1,056 ± 251	2,007 ± 202
Typical	9	13,707 ± 1,447	3,761 ± 331	77 ± 4	49 ± 3	2,814 ± 249	0.75 ± 0.05	386 ± 13	986 ± 148
Visual									
Bitufted	3	19,334 ± 2,944	4,928 ± 644	79 ± 2	63 ± 9	3,434 ± 266	0.73 ± 0.14	448 ± 54	1,464 ± 229
Extraverted	5	9,183 ± 889	2,386 ± 370	65 ± 8	38 ± 5	1,583 ± 492	0.63 ± 0.15	342 ± 36	730 ± 173
Horizontal	4	14,636 ± 3,558	4,837 ± 1,056	94 ± 4	51 ± 11	2,982 ± 694	0.66 ± 0.10	377 ± 65	1,328 ± 343
Inverted	4	12,188 ± 1,293	3,128 ± 412	75 ± 9	43 ± 6	1,345 ± 489	0.43 ± 0.14	510 ± 92	1,457 ± 287
Magnopyramidal	3	26,702 ± 9,657	4,062 ± 740	93 ± 3	44 ± 9	2,757 ± 548	0.68 ± 0.02	734 ± 267	2,216 ± 134
Multiapical	1	19,894	3,190	60	53	2,111	0.66	514	2,218
Typical	16	14,606 ± 1,357	3,771 ± 307	77 ± 3	49 ± 3	2,436 ± 232	0.65 ± 0.03	368 ± 26	1,414 ± 156
<i>Humpback whale</i>									
Anterior temporal									
Extraverted	6	19,509 ± 1,962	4,454 ± 365	97 ± 4	46 ± 4	2,479 ± 266	0.55 ± 0.03	593 ± 56	1,001 ± 185
Horizontal	2	42,153 ± 5,923	6,056 ± 1,108	84 ± 9	72 ± 6	2,553 ± 569	0.42 ± 0.02	747 ± 61	1,941 ± 4
Magnopyramidal	5	56,006 ± 7,225	9,602 ± 781	98 ± 2	98 ± 7	5,054 ± 324	0.54 ± 0.04	1,172 ± 183	1,587 ± 54
Typical	4	19,911 ± 3,517	4,709 ± 749	78 ± 7	60 ± 7	2,588 ± 286	0.57 ± 0.06	542 ± 51	973 ± 112
Stemzelle	2	25,669 ± 1,438	6,726 ± 625	96 ± 13	72 ± 16	2,922 ± 212	0.44 ± 0.01	921 ± 25	2,044 ± 10

Table 1 continued

Type	n^a	Vol. ^b	TDL ^c	MSL ^c	DSC ^d	DSN ^e	DSD ^f	SoSize ^e	SoDepth ^h
Frontal									
Extraverted	8	20,798 ± 2,039	4,499 ± 508	83 ± 5	54 ± 5	2,210 ± 401	0.49 ± 0.06	475 ± 34	1,297 ± 148
Magnopyramidal	5	38,681 ± 2,744	8,031 ± 1,131	104 ± 2	78 ± 11	5,085 ± 750	0.64 ± 0.07	745 ± 44	1,681 ± 49
Multipolar	3	27,238 ± 8,368	5,125 ± 479	87 ± 8	59 ± 2	3,083 ± 844	0.58 ± 0.12	458 ± 36	1,327 ± 191
Typical	5	23,249 ± 1,449	5,645 ± 508	80 ± 8	71 ± 7	3,388 ± 474	0.60 ± 0.06	543 ± 57	1,043 ± 96
Sternzelle	3	34,750 ± 8,504	6,243 ± 1,714	98 ± 16	63 ± 12	4,031 ± 1,597	0.61 ± 0.07	668 ± 118	1,624 ± 187
Posterior temporal									
Bitufted	1	15,165	4,586	100	46	3,394	0.74	416	1,708
Horizontal	1	22,642	4,871	67	73	1,539	0.32	711	1,980
Magnopyramidal	6	54,547 ± 11,880	8,255 ± 642	104 ± 7	80 ± 4	3,612 ± 857	0.43 ± 0.08	933 ± 99	1,862 ± 212
Typical	2	27,738 ± 10,750	5,231 ± 2,326	85 ± 14	59 ± 18	1,822 ± 324	0.40 ± 0.12	568 ± 127	1,614 ± 185
Sternzelle	3	33,694 ± 1,882	6,408 ± 451	91 ± 5	70 ± 1	2,105 ± 198	0.33 ± 0.02	1,005 ± 46	2,262 ± 81
Visual									
Extraverted	4	13,936 ± 4,557	2,230 ± 717	56 ± 11	38 ± 5	1,133 ± 285	0.53 ± 0.08	529 ± 90	1,044 ± 287
Horizontal	1	31,858	8,399	79	106	3,381	0.40	766	2,213
Magnopyramidal	11	63,052 ± 7,970	9,394 ± 410	107 ± 6	89 ± 5	4,826 ± 414	0.52 ± 0.04	1,103 ± 157	1,756 ± 72
Typical	9	22,127 ± 1,803	5,892 ± 563	76 ± 4	79 ± 8	3,682 ± 468	0.62 ± 0.05	495 ± 23	1,236 ± 115
Aspiny neurons									
<i>Bottlenose dolphin</i>									
Anterior temporal									
Multipolar	1	3,135	1,532	77	20	29	0.02	297	960
Visual									
Multipolar	1	18,107	4,062	77	53	1,231	0.30	519	860
<i>Minke whale</i>									
Visual									
Bipolar	1	2,313	1,235	54	23	27	0.02	256	936
Multipolar	2	5,470 ± 1,068	2,217 ± 742	68 ± 9	32 ± 7	38 ± 5	0.02	392 ± 41	1,059 ± 52

^a Number of cells traced^b Volume in μm^3 ^c Length in μm ^d Number of segments per neuron^e Number of spines per neuron^f Number of spines per μm of dendritic length^g Soma size in μm^2 ^h Soma depth in μm from the pial surface

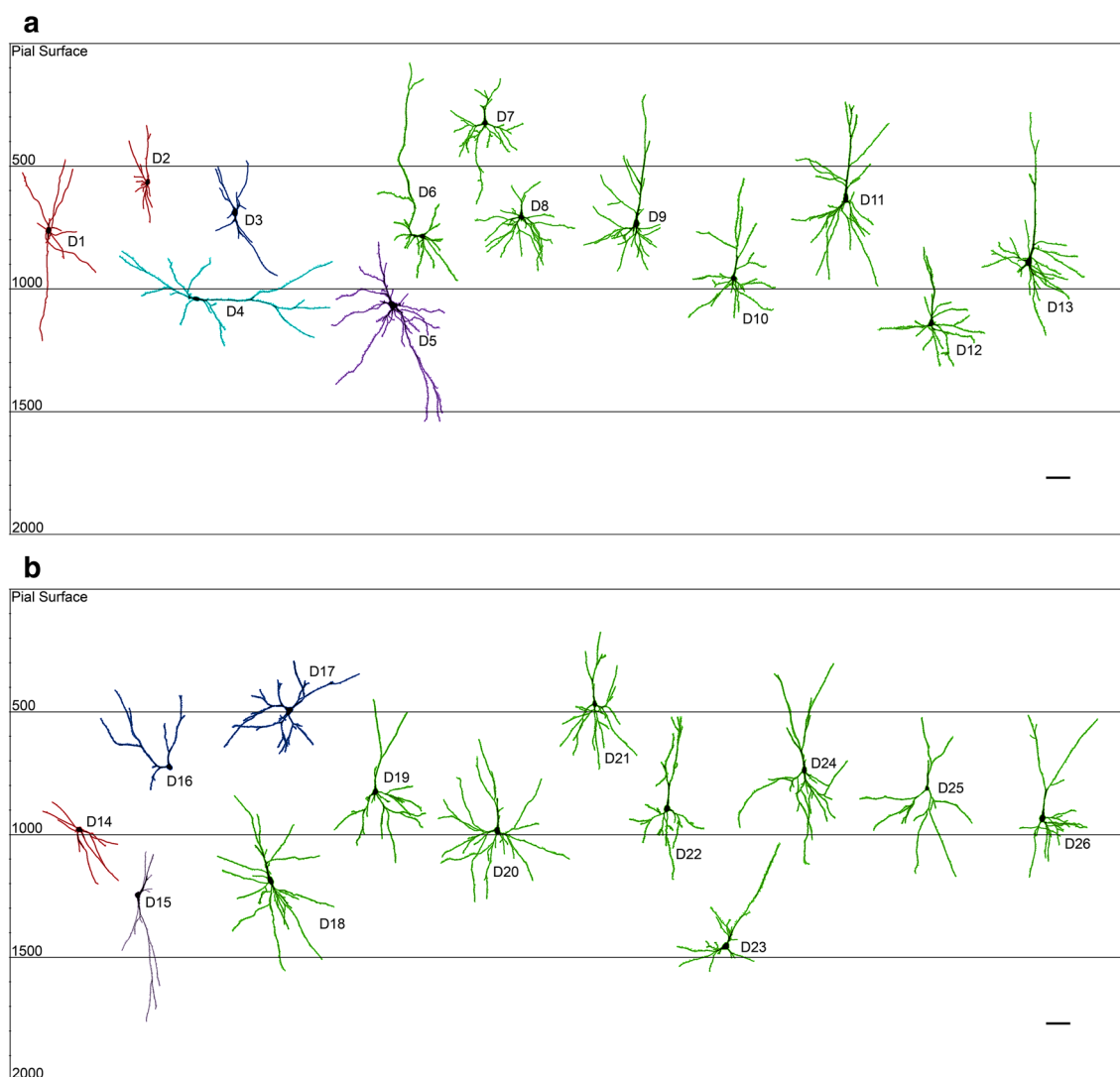


Fig. 7 NeuroLucida tracings of neurons in the bottlenose dolphin visual (a) and anterior temporal (b) cortices, arranged by their soma depth from the pial surface (in μm). Visual cortex (a): aspiny multipolar neurons (D1, D2); extraverted pyramidal neuron (D3); flattened pyramidal neuron (D4); magnopyramidal neuron (D5); and

typical pyramidal neurons (D6–D13, D11 tri-tufted variant). Anterior temporal cortex (b): aspiny multipolar neuron (D14); bitufted pyramidal neuron (D15); extraverted pyramidal neurons (D16, D17); and typical pyramidal neurons (D18–D26); and two tri-tufted variants (D23, D25). Scale bar 100 μm

extensive apical branching and underdeveloped basilar skirts (only 2.94 ± 1.86 primary branches per extraverted neuron compared to 4.85 ± 2.06 for typical pyramidal neurons). More specifically, comparison of extraverted ($n = 22$) and typical pyramidal ($n = 47$) neurons with relatively complete apical dendrites revealed that apical dendrite TDL was 15 % greater in extraverted neurons ($2,176 \mu\text{m}$) than in typical pyramidal neurons ($1,839 \mu\text{m}$), but basilar dendrite TDL was 48 % greater in typical pyramidal neurons ($2,502 \mu\text{m}$) over extraverted neurons ($1,310 \mu\text{m}$). Average DSD varied from 0.07 to and 0.63 (Table 1). Sholl analyses revealed that apical dendritic density was equal to or greater than that of the basilar skirts (Fig. 11).

As with the typical pyramidal neurons, only extraverted pyramidal neurons with relatively complete apical dendrites were analyzed inferentially (bottlenose dolphin, $n = 6$; minke whale, $n = 5$; humpback whale, $n = 11$). Overall, significant species differences were obtained on three of the four dependent variables even after factoring out soma depth, revealing the following pattern: humpback whale > minke whale > bottlenose dolphin (Fig. 14). Humpback whale Vol was 104.0 % greater than that of the minke whale and 187.0 % greater than that of the bottlenose dolphin ($F_{(2,18)} = 19.52$, $p < 0.05$, $\eta_p^2 = 0.684$). TDL in the humpback whale was 77.0 % greater than that of the minke whale and 117.4 % greater than that of the bottlenose dolphin ($F_{(2,18)} = 9.96$, $p < 0.05$, $\eta_p^2 = 0.525$).

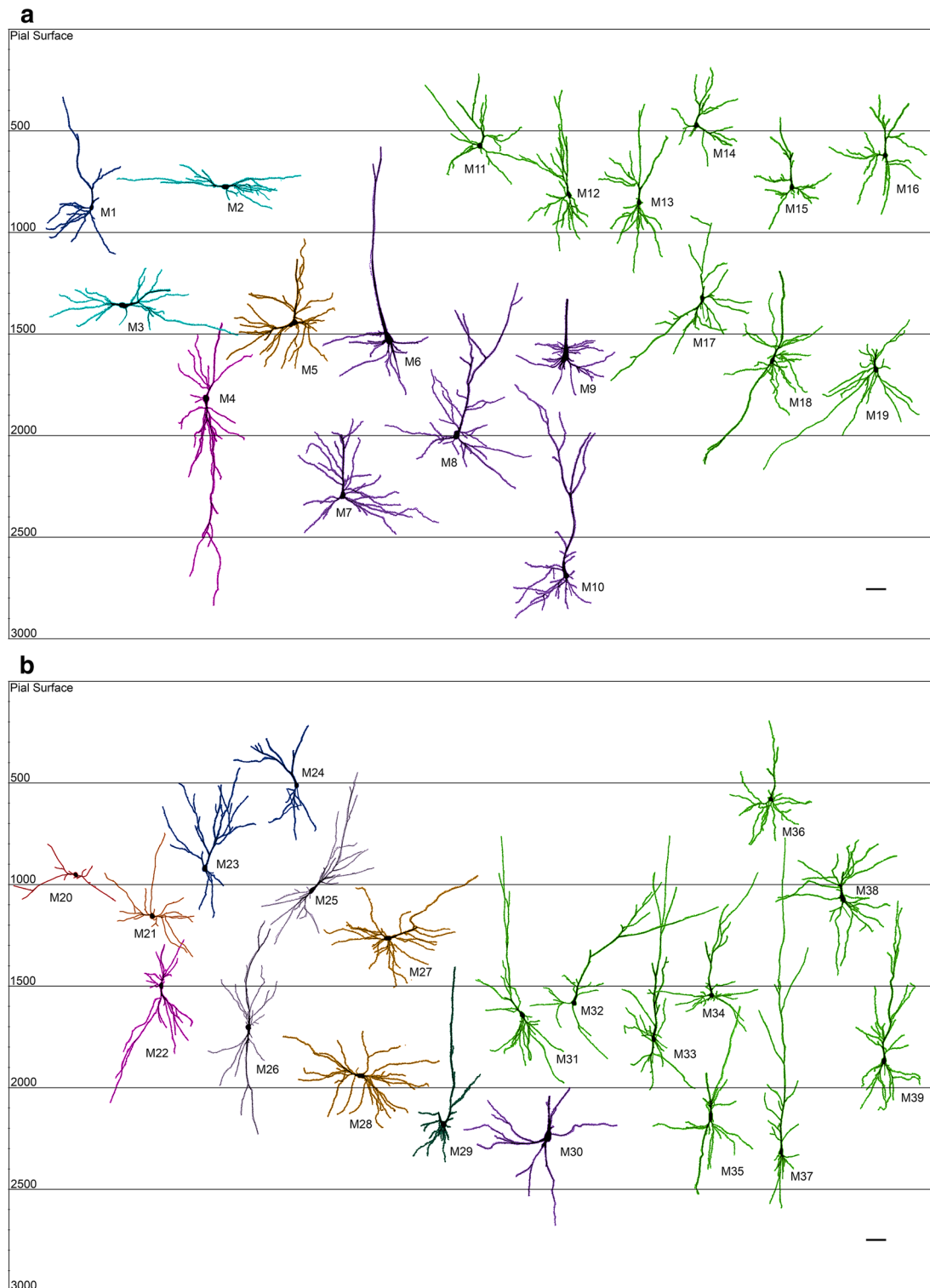


Fig. 8 NeuroLucida tracings of neurons in the minke whale motor (a) and visual (b) cortices, arranged by their soma depth from the pial surface (in μm). Motor cortex (a): extrverted pyramidal neuron (M1); flattened pyramidal neurons (M2–M3); inverted pyramidal neuron (M4); horizontal pyramidal neuron (M5); magnopyramidal neurons (M6–M10); and typical pyramidal neurons (M11–M19).

Visual cortex (b): aspiny bipolar neuron (M20); aspiny multipolar neuron (M21); inverted pyramidal neuron (M22); extrverted pyramidal neurons (M23, M24); bitufted pyramidal neurons (M25, M26); horizontal pyramidal neurons (M27, M28); multipical pyramidal neuron (M29); magnopyramidal neuron (M30); and typical pyramidal neurons (M31–M39). Scale bar 100 μm

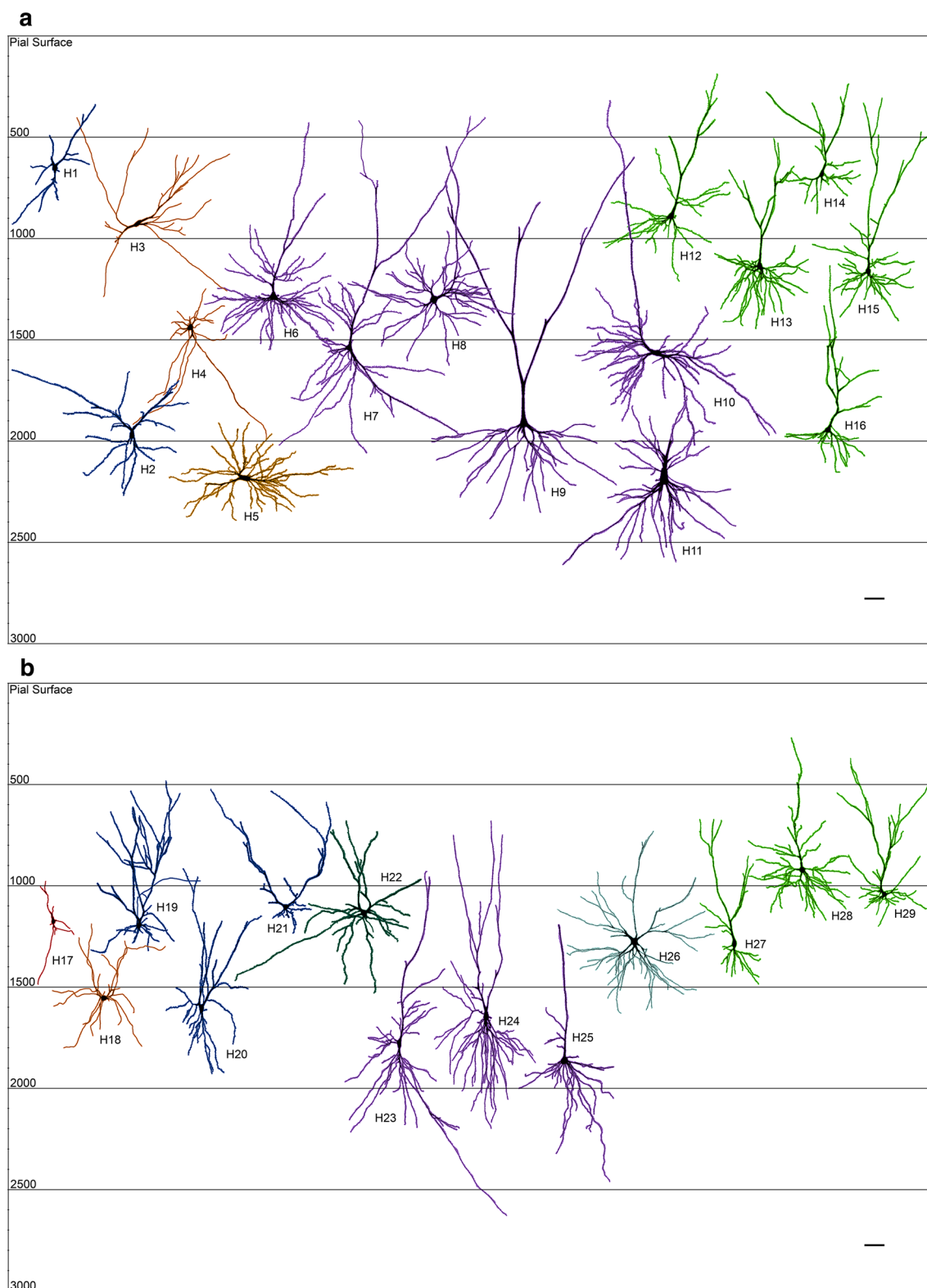


Fig. 9 NeuroLucida tracings of neurons in the humpback whale visual (**a**) and frontal (**b**) cortices, arranged by their soma depth from the pial surface (in μm). Visual cortex (**a**): extraverted pyramidal neurons (*H1*, *H2*); aspiny multipolar neurons (*H3*, *H4*); horizontal pyramidal neuron (*H5*); magnopyramidal neurons (*H6*–*H11*, *H7* tri-tufted variant); and typical pyramidal neurons (*H12*–*H16*). Frontal cortex

(**b**): aspiny bipolar neuron (*H17*); aspiny multipolar neuron (*H18*); extraverted pyramidal neurons (*H19*–*H21*); multiapical pyramidal neuron (*H22*); magnopyramidal neurons (*H23*–*H25*, *H23* tri-tufted variant); Sternzellen (*H26*); and typical pyramidal neurons (*H27*–*H29*, *H27* tri-tufted variant). Scale bar 100 μm

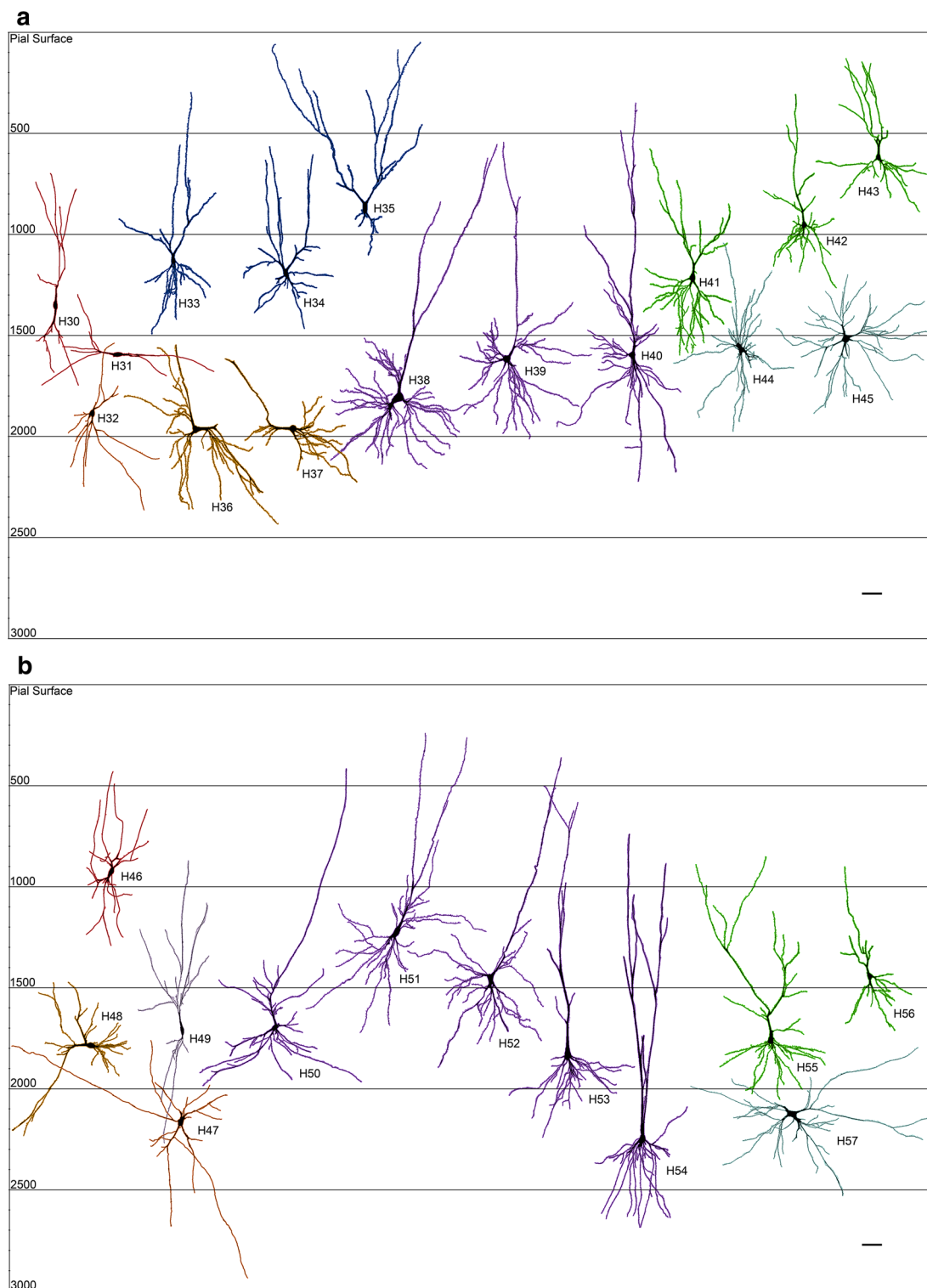


Fig. 10 NeuroLucida tracings of neurons in the humpback whale anterior (a) and posterior (b) temporal cortices, arranged by their soma depth from the pial surface (in μm). Anterior temporal cortex (a): aspiny bipolar neurons (H30, H31); aspiny multipolar neuron (H32); extrverted pyramidal neurons (H33–H35); horizontal pyramidal neurons (H36, H37); magnopyramidal neurons (H38–H40, H38, H40 tri-tufted variants); typical pyramidal neurons (H41–H43);

and Sternzellen (H44, H45). Posterior temporal cortex (b): aspiny bipolar neuron (H46); aspiny multipolar neuron (H47); horizontal pyramidal neuron (H48); bitufted pyramidal neuron (H49); magnopyramidal neurons (H50–H54, H52 tri-tufted variant); typical pyramidal neurons (H55–H56, H56 tri-tufted variant), and Sternzellen (H57). Scale bar 100 μm

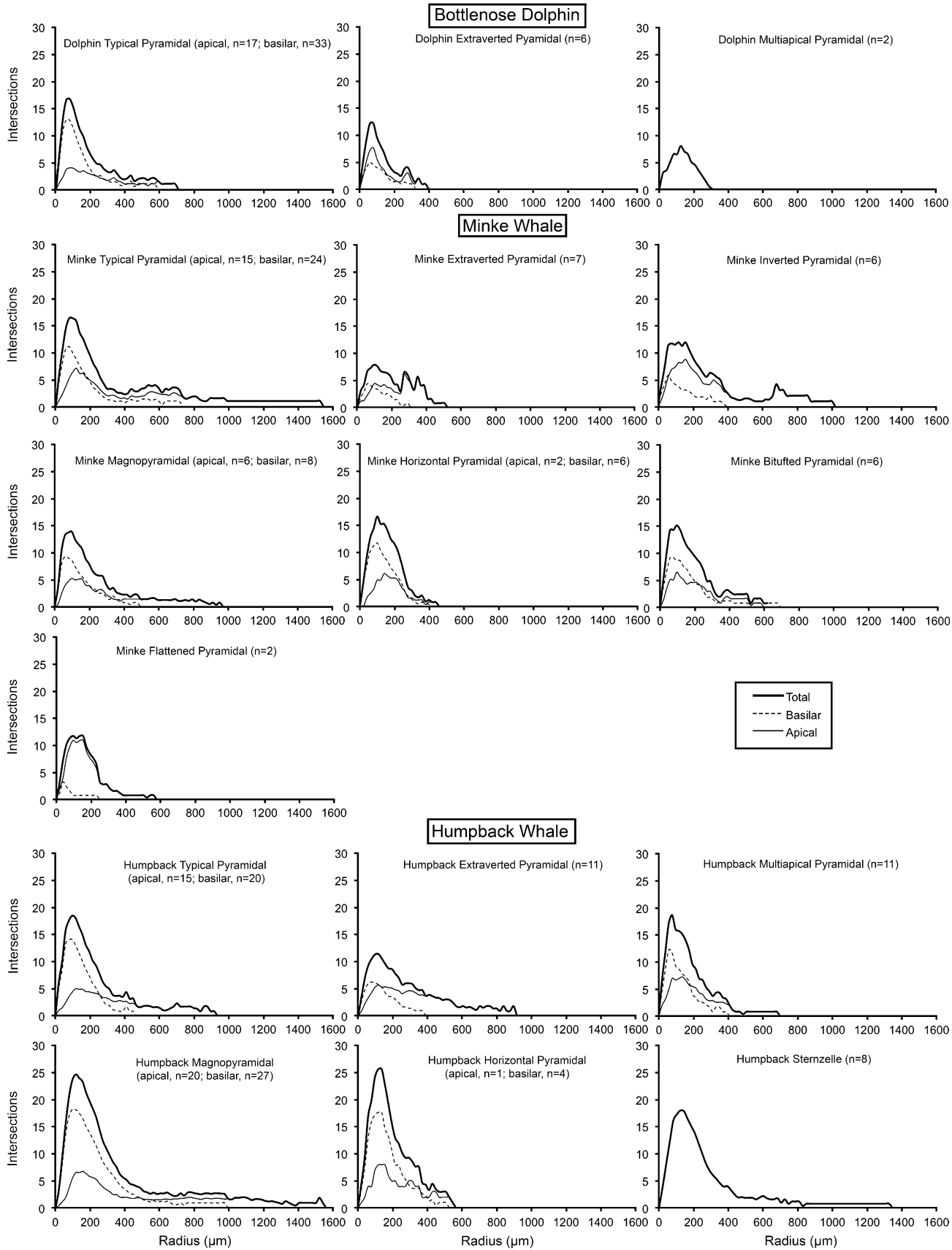


Fig. 11 Sholl analysis of spiny neurons in the three cetacean species. Sholl analysis assesses the relative complexity of the basilar, apical, and total dendritic branching patterns, using concentric rings spaced at 20 μm that measure dendritic intersections. The figure shows that for typical pyramidal neurons across all three species, basilar density peaked before, and was much higher than, apical density; the same holds true for minke whale and humpback whale magnopyramidal neurons. For extraverted pyramidal neurons across all three species, apical density was equal to or higher than basilar density

Humpback whale MSL was 42.0 % greater than that of the minke whale and 75.6 % greater than that of the bottlenose dolphin ($F_{(2,18)} = 9.32$, $p < 0.05$, $\eta_p^2 = 0.509$). No significant differences were found between the bottlenose dolphin and the minke whale, indicating that extraverted pyramidal neurons in the humpback whale had significantly greater Vol, TDL, and MSL than those observed in the other two species. No significant species differences obtained for DSC, indicating that the extraverted pyramidal neurons exhibited a similar number of dendritic segments across the three species.

Magnopyramidal neurons ($n = 36$; soma depth range 1,084–2,216 μm ; Table 1) were located in most cortical areas (Fig. 7a: D5; Fig. 8a: M6–10; Fig. 8b: M30; Fig. 9a: H6–11; Fig. 9b: H23–25; Fig. 10a: H38–40; Fig. 10b: H50–54), except for the anterior temporal cortex of the bottlenose dolphin. They were morphologically similar to

typical pyramidal neurons but were much larger in terms of Vol (by 72 %), TDL (by 50 %), MSL (by 32 %), DSC (by 28 %), and soma size (by 59 %). Magnopyramidal neurons appeared to have more vertically oriented and more widely bifurcating apical dendrites than did typical pyramidal neurons (Figs. 4d, 5a, b). The pattern and number of apical bifurcations varied among individual neurons, with some apical dendrites bifurcating in V-shaped formations (Fig. 9a: H9; Fig. 9b: H24) and others displaying a single apical shaft that extended for several hundred micrometers before its first bifurcation (Fig. 8a: M6). With an average of 6.25 ± 3.32 primary basilar dendrites per neuron, their basilar skirt pattern varied according to soma shape: those with rounded and triangular somata exhibited basilar dendritic fields that surrounded the cell body (Fig. 9a: H6, H8; Fig. 9b: H25), whereas those with elongated somata exhibited basilar dendritic fields that extended in a more vertical manner towards the white matter (Fig. 9b: H23, H24). Similar to typical pyramidal neurons, some magnopyramidal neurons possessed a tri-tufted morphology, with an apical dendrite and two thick basilar dendrites emerging from the soma at 90° angles (Fig. 5c, d; Fig. 9a: H7, H10; Fig. 9b: H23; Fig. 10a: H38, H40). Average DSD of magnopyramidal neurons (0.55) was slightly higher (by 15.0 %) than that of typical pyramidal neurons (0.47). Sholl analysis of magnopyramidal neurons revealed the

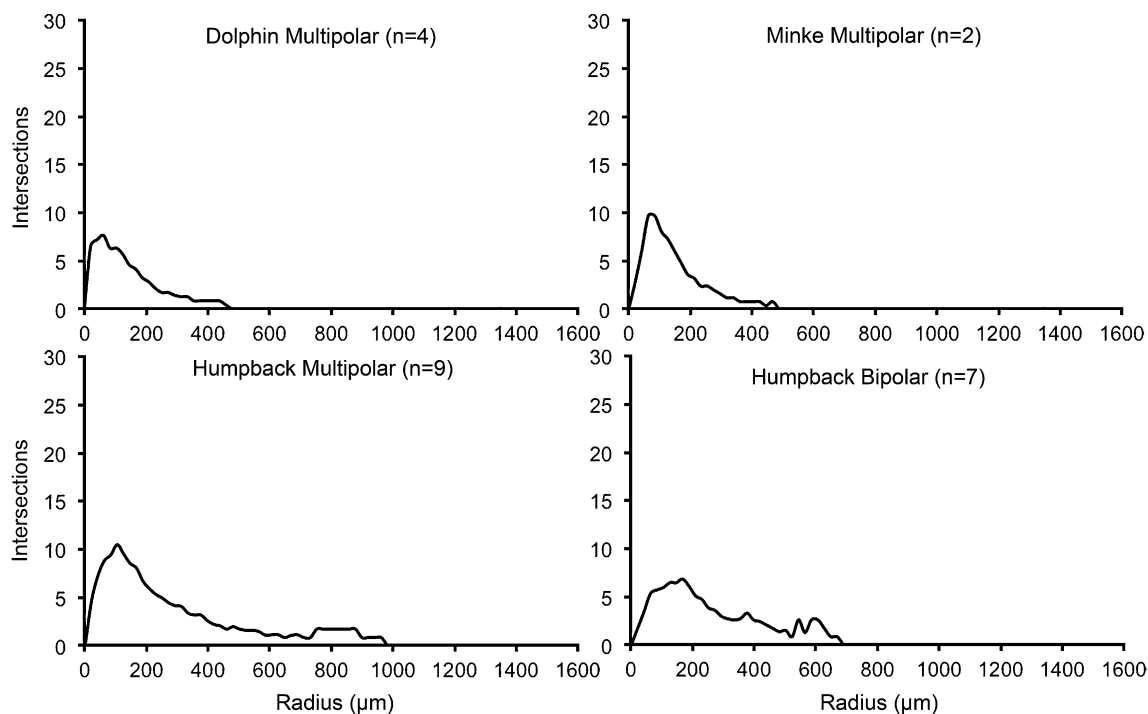


Fig. 12 Sholl analysis of aspiny neuronal types in the three cetacean species. Sholl analysis assesses the relative complexity of the basilar, apical, and total dendritic branching patterns, using concentric rings

spaced at 20 μm to measure dendritic intersections. The figure shows that both aspiny neuronal morphologies show a peak of dendritic density close to the soma

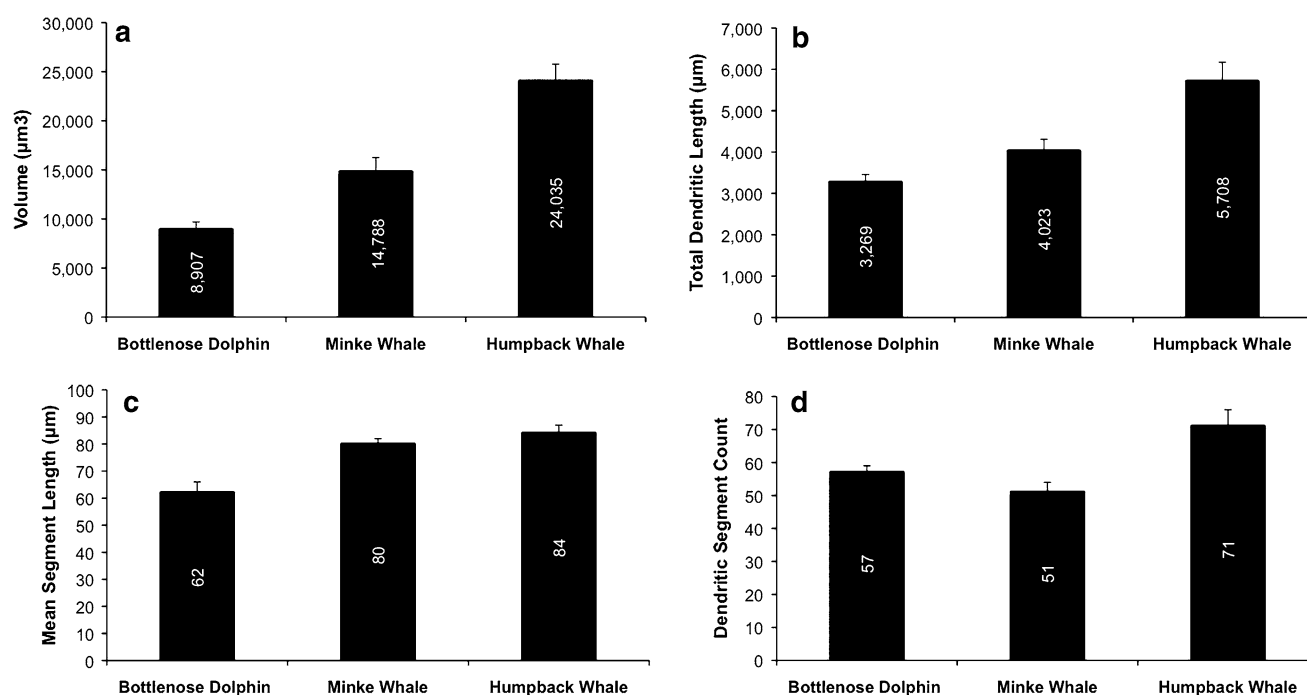


Fig. 13 Bar graphs of relative volume (a), total dendritic length (b), mean segment length (c), and dendritic segment count (d) of typical pyramidal neurons in the bottlenose dolphin, minke whale, and

humpback whale. In general, measures increased from dolphin to minke whale to humpback whale, except for dendritic segment count. Error bars represent SEM

basilar skirt to be more dense and apical branches to be much longer than observed in most other neuron types (Fig. 11).

Multiapical pyramidal neurons ($n = 6$; soma depth range 630–2,218 μm ; Table 1) were observed in the bottlenose dolphin anterior temporal ($n = 1$) and visual ($n = 1$) cortices, the minke whale visual cortex ($n = 1$, Fig. 8b: M29), and the humpback whale frontal cortex ($n = 3$, Fig. 9b: H22). These neurons were characterized by two or more distinct apical dendrites that extended from the soma toward the pial surface and well-developed basilar skirts (average 5.0 ± 2.53 primary basilar dendrites per neuron) that extended mainly towards the white matter. Their average DSD ranged from 0.30 to 0.66. Multiapical pyramidal neurons were differentiated from extraverted pyramidal neurons in that multiapical neurons possessed an extensive basilar skirt similar to that of a typical pyramidal neuron. A Sholl analysis revealed small multiapical pyramidal neurons in the bottlenose dolphin with incomplete basilar skirts and short, low-density apical dendrites (Fig. 11). Multiapical pyramidal neurons in the humpback whale had denser and longer apical dendrites than basilar dendrites, both having relatively high peaks close to the soma. Because only one multiapical pyramidal neuron was found in the minke whale, no Sholl Analysis was performed.

Bitufted pyramidal neurons ($n = 5$; soma depth range 1,232–1,708 μm ; Fig. 7b: D15; Table 1) were located in

the anterior temporal cortex of the bottlenose dolphin ($n = 1$, Fig. 7b: D15), the visual cortex of the minke whale ($n = 3$, Fig. 8b: M25, M26), and the posterior temporal cortex of the humpback whale ($n = 1$, Fig. 10b: H49). These neurons possessed rounded or elongated somata with apical dendrites that ascended towards the pia mater and basilar dendrites (2.8 ± 1.3 primary basilar branches per neuron) that descended towards the white matter (Fig. 3e). DSD was between 0.40 and 0.74. Consistent with the majority of neuronal types, the Sholl analysis for bitufted pyramidal neurons revealed a higher density of basilar than apical dendrites; both basilar and apical dendritic density peaked close to the soma with branching extending somatofugally for a similar distance (Fig. 11).

Atypical pyramidal neurons

Inverted pyramidal neurons ($n = 5$; soma depth range 1,457–1,810 μm ; see Table 1) were found only in the minke whale motor ($n = 1$, Fig. 8a: M4) and visual ($n = 4$, Fig. 8b: M22) cortices. Although morphologically similar to typical pyramidal neurons, the inverted pyramidal neurons were oriented such that the apical dendrite descended towards white matter and the basilar skirt (2.4 ± 1.14 primary basilar branches per neuron), projected laterally and towards the pial surface (Fig. 4b). The inverted pyramidal neuron in the motor cortex was larger

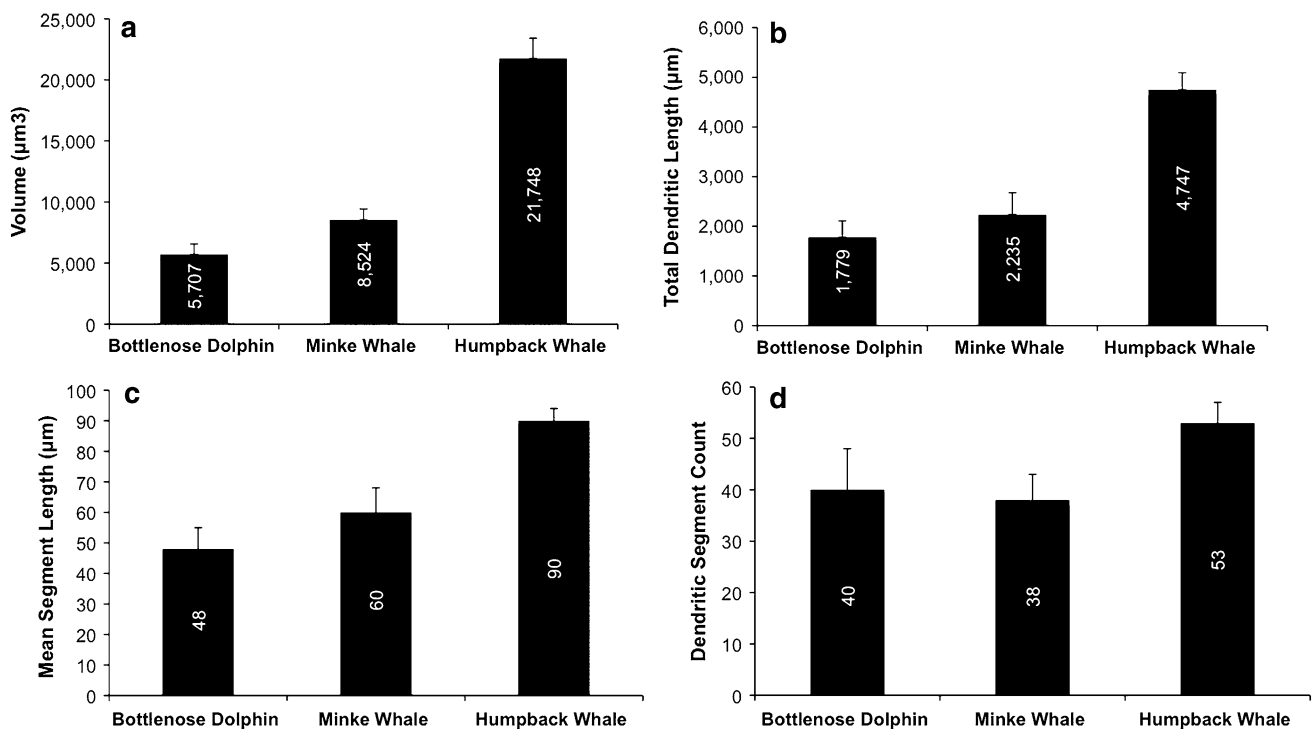


Fig. 14 Bar graphs of relative volume (a), total dendritic length (b), mean segment length (c), and dendritic segment count (d) of extraverterted pyramidal neurons in the bottlenose dolphin, minke whale, and humpback whale. For graphs a–c, the dependent measures

of Volume, TDL, and MSL were significantly greater in the humpback whale than in the bottlenose dolphin and the minke whale. Error bars represent SEM

than those in the visual cortex. Average DSD ranged from 0.43 to 0.90. In the Sholl analysis, dendritic density peaks were close to the soma, with apical dendritic density peaking slightly higher and further from the soma than basilar dendrites (Fig. 11).

Horizontal pyramidal neurons ($n = 10$; soma depth range 1,328–2,481 µm; Table 1) were found in the minke whale visual ($n = 4$, Fig. 8a: M5) and motor ($n = 2$, Fig. 8b: M27, M28) cortices and in humpback whale visual ($n = 1$, Fig. 9a: H5), anterior temporal ($n = 2$, Fig. 10a: H36, H37) and posterior temporal ($n = 1$, Fig. 10b: H48) cortices. Somata shape varied from triangular to square, elongated, or round. Apical dendrites extended laterally or obliquely ($<45^\circ$) instead of perpendicularly (Fig. 4f), and dense basilar skirts (5.2 ± 1.99 primary basilar branches per neuron) extended around the soma in all directions. Average DSD ranged from 0.32 to 0.81. Sholl analysis revealed that maximum dendritic density peaked close to the soma, and that basilar dendrites were denser and longer in the humpback whale than in the minke whale (Fig. 11).

Flattened pyramidal neurons ($n = 4$; soma depth range 864–1,090 µm; Table 1) were found in the bottlenose dolphin visual ($n = 2$, Fig. 7a: D4) and minke whale motor ($n = 2$, Fig. 8a: M2, M3) cortices. Two apical shafts with shallow, acute bifurcations protruded horizontally from opposite ends of the soma, eventually orienting towards the

pial surface. Basilar dendrites were minimal (1.33 ± 0.58 primary basilar branches per neuron) and descended towards the white matter alongside the apical dendrites (Fig. 4g). DSD ranged from 0.26 to 0.57. Because apical dendrites of flattened pyramidal neurons in the bottlenose dolphin were incomplete, the Sholl analysis was only performed on the two minke whale neurons. This analysis revealed that apical dendrites were much denser and longer than basilar dendrites (Fig. 11).

Nonpyramidal spiny neurons

Sternzellen ($n = 8$; soma depth range 1,624–2,262 µm; Table 1), first named by (Kraus and Pilleri 1969b), were located in the deeper cortical layers of humpback whale frontal ($n = 3$, Fig. 9b: H26), anterior temporal ($n = 2$, Fig. 10a: H44, H45), and posterior temporal ($n = 3$, Fig. 10b: H57) cortices. These neurons possess a star-like appearance, with multiple, similarly sized dendrites emerging from several points on a rounded or square-like soma. An average of 6.5 ± 3.21 primary dendrites extended in all directions, creating a circular dendritic field with no discernible apical dendrite (Fig. 5d). Their average DSD ranged from 0.33 to 0.61. Sternzellen quantified in humpback whale frontal cortex had more spines, smaller somata, and were more superficial than those located in

other cortical areas. Sholl analyses revealed a relatively large dendritic density near the soma and relatively long projections from the soma similar to those of typical pyramidal neurons in the humpback whale (Fig. 11).

Aspiny neurons

Aspiny neurons were generally smaller and less complex than spiny neurons, with fewer dendritic branches, and lower dependent measures when compared to spiny neurons (Table 1). Aspiny interneurons in the current sample included bipolar and multipolar neurons.

Bipolar neurons ($n = 8$; soma depth range 924–1,469 μm ; Table 1) were observed in the visual cortex of the minke whale ($n = 1$, Fig. 8a: M20) and the frontal ($n = 1$, Fig. 9a: H17), anterior temporal ($n = 5$), and posterior temporal ($n = 1$, Fig. 10b: H46) cortices of the humpback whale. These neurons were characterized by rounded or oblong somata with an average of 3.0 ± 1.31 dendrites extending out either horizontally or vertically from opposite poles (Fig. 5f). A Sholl analysis of bipolar neurons in the humpback whale revealed an elongated peak in dendritic density near the soma and moderately long dendrites that extended approximately 700 μm somatofugally (Fig. 12). The mean dendritic radius of bipolar neurons was 469 μm in the humpback whale and 300 μm in the minke whale. Aspiny bipolar neurons in the bottlenose dolphin did not stain completely enough to be traced.

Multipolar neurons ($n = 15$; soma depth range 781–1,854 μm ; Table 1) were found in most cortical areas (Fig. 7a: D1, D2; Fig. 7b: D14; Fig. 8b: M21; Fig. 9a: H3, H4; Fig. 9b: H18; Fig. 10a: H32; Fig. 10b: H47) except for the minke whale motor cortex. These neurons were characterized by an average of five dendrites that extended radially in all directions from the soma (Fig. 3c). Sholl analyses revealed that dendritic density peaked very close to the soma, at less than 200 μm (Fig. 12). The mean dendritic radius of multipolar neurons was 575 μm in the humpback whale, 375 μm in the minke whale, and 300 μm in the bottlenose dolphin.

Discussion

Studies of neuronal morphology in cetaceans are few (e.g., striped dolphin: Ferrer and Perera 1988; bottlenose dolphin: Garey et al. 1985; short-beaked common dolphin, *Delphinus delphis*: Kraus and Pilleri 1969b), with only one neuromorphological study in mysticetes (sei whale: Kraus and Pilleri 1969b, c). The present study provides descriptions and quantitative data on neuronal morphology in one odontocete and two mysticetes. The variety of neuronal types documented here suggests that cetaceans possess a

range of neuronal morphologies similar to that seen in many terrestrial mammals (de Lima et al. 1990; Jacobs et al. 2011, 2014a). Moreover, a prominent characteristic of many cetacean spiny neurons was the frequent bifurcation of apical dendrites, a characteristic similar to that observed in other cetartiodactyls (Jacobs et al. 2014a). Two morphologies were particularly apparent in cetaceans: tri-tufted pyramidal neurons and Sternzellen. Although the morphological characteristics of neurons were consistent across all species, cross-species comparisons indicated that both typical pyramidal and extraverted neurons increased in dendritic extent from the bottlenose dolphin to the humpback whale.

Methodological considerations

Generally, the same limitations that apply to Golgi studies on human brain materials apply to the present tissue (Jacobs et al. 2011, 2014b; Jacobs and Scheibel 2002). Instead of focusing on these well-established issues, we review here those particularly relevant to the current study, namely the effects of differential fixation time on Golgi impregnations, the question of functional classification of cetacean cortical regions, and issues of neuronal classification (Bota and Swanson 2007; Germroth et al. 1989; Masland 2004) based solely on somatodendritic architecture (Ascoli et al. 2008). Finally, we briefly discuss the issue of using species of different ages in neuromorphological studies.

Fixation time

Although the importance of short autolysis times for high-quality Golgi impregnations is generally accepted (de Ruiter 1983), there appears to be little consensus on the effects of fixation time (Buell 1982; Williams et al. 1978). In our own work on the human brain, we have found a fixation time of 2–3 months to be optimal for the modified rapid Golgi technique (Anderson et al. 2009). In the present study, it was not possible to control such factors, and the prolonged fixation times (>6 months) for minke whale and dolphin brains may have resulted in suboptimal fixation when compared to the humpback whale tissue. For this and perhaps other reasons, dendritic extent and especially spine density appeared reduced in the bottlenose dolphin brain. Consequently, we did not perform quantitative comparisons of spine measurements among the three species.

Functional classification of cortical regions

Although the anatomy of the cetacean brain has been extensively investigated, much less is known about functional localization among cetacean species beyond basic

sensory functions in the bottlenose dolphin (Ladygina et al. 1978; Ladygina and Supin 1977). Furthermore, observations of the cerebral cortex of minke whale and humpback whale have been limited to cytoarchitecture. Moreover, in these species, functional localization is generally presumed from their cytoarchitecture and from electrophysiological studies in the bottlenose dolphin (Eriksen and Pakkenberg 2007; Hof and Van der Gucht 2007; Ladygina et al. 1978; Ladygina and Supin 1977). As such, although the present study provides observations about the regional distribution of traced neurons, our findings cannot be related to specific cortical functions. Therefore, it was impossible to correlate dendritic or spine parameters with the functional attributes of the sampled regions, as has been done in primates (Elston and Rosa 1998a, b; Jacobs et al. 2001).

Neuronal classification

Although neuronal classification is essential for elucidating the relationship between structure and function, the process is confounded because neuronal characterizations in the literature are often ambiguous, contradictory, and/or change over time (DeFelipe et al. 2013; Ferrer and Perera 1988; Garey et al. 1985; Glezer and Morgane 1990; Masland 2004). Classification is further limited when neurons are described solely according to somatodendritic measures without information on axonal morphology, as is the case in the present investigation. Additional issues are faced in comparative studies, given the lack of an official comparative nomenclature. In fact, the template against which all other brains are compared and that defines what is “typical” versus what is “atypical” is represented by few species of primates and rodents and actually does not necessarily represent the major clades of mammals (DeFelipe et al. 2013; Manger et al. 2008; Sherwood et al. 2009). For consistency, the present investigation attempted to follow existing nomenclature (Ferrer and Perera 1988; Jacobs et al. 2011) in classifying pyramidal neurons as a neuronal type under which several variations exist along a continuum. Although we observed many examples of the described neuron types in our Golgi-stained sections, we only traced those that were relatively complete and unobscured, which limited our overall conclusions regarding neuronal classes.

Effect of age on neuronal morphology

It is recognized that, in primates, age has an influence on the size of basal dendritic trees in pyramidal neurons of different cortical areas (Jacobs and Scheibel 1993; Jacobs et al. 1997). Particularly, in macaque monkeys, while pyramidal neurons of some cortical regions (e.g., inferotemporal and prefrontal cortex) continue to grow larger

basal dendritic trees into adulthood (Cupp and Uemura 1980; Elston et al. 2009, 2010a), in other areas (e.g., primary visual and primary auditory), the increase in age is related to a decrease in the size of basal dendritic trees (Boothe et al. 1979; Elston et al. 2010a, b). Moreover, there are differences in branching complexity and growth rate across different neuronal populations (Elston et al. 2011). Such heterogeneity of growth patterns has been related to genetic and epigenetic mechanisms regulating neuronal growth differently across cortical areas and linking different growth profiles to the function performed by the neuron in the adult brain (Elston et al. 2011).

Ideally, studies of quantitative neuronal morphology attempting to unravel details of connectivity and circuitry in the developing and mature neocortex, should include only specimens of comparable ages. As is often the case in comparative studies such as the present, however, it was not possible to control for the age of the specimens. The quantitative measures obtained from the young humpback whale specimen could thus be different from the same measures recorded in an adult. However, our previous examination of neuronal morphology in humans suggests that fundamental differences in neuronal types do not appear to be age-specific, although quantitative changes in dendritic measures certainly do obtain (Jacobs and Scheibel 1993; Jacobs et al. 1997; Travis et al. 2005). As such, the present study still provides an overview of neuronal morphologies for the sampled species that can be used as reference in future comparative studies.

Spiny neurons

Pyramidal-like neurons

In the present sample, there was considerable heterogeneity of spiny neuron morphologies, many of which have already been described in terrestrial mammals (Jacobs et al. 2011; Meyer 1987; Sherwood et al. 2009).

In accordance with rodent and primate models, the spiny neurons observed in the present study included three major classes: (1) pyramidal-like neurons; (2) neurons with “atypical” orientations and bifurcations of the apical dendrite; (3) and neurons without a discernable apical dendrite.

Typical pyramidal neurons were the predominant neuron type observed throughout the cortical layers. In general, typical pyramidal neurons were comparable to primate and rodent pyramidal neurons by virtue of their thick, ascending apical dendrite and their well-developed basilar skirt. Two main variations of apical dendrites were observed: a straight apical shaft that ascended for a long distance before bifurcating and an apical dendrite that divided into two dendritic branches shortly after leaving the soma, resulting in a V-shaped apical dendrite. This

second variation is similar to the bifurcating apical dendrites observed in the pygmy hippopotamus (Butti et al. 2014) and the giraffe (Jacobs et al. 2014a), but is less widely bifurcating than those described in the African elephant (Jacobs et al. 2011). The presence of the tri-tufted variant across cetacean species and cortical regions suggests that this neuronal type may be a unique feature of this lineage (Ferrer and Perera 1988; Garey et al. 1985). Notably, in our recent Golgi investigation of the pygmy hippopotamus cortex, we failed to observe this tri-tufted variant (Butti et al. 2014). Thus, more comparative neuromorphological investigations are required to determine if this neuronal morphology exists in other non-cetacean species.

Extraverted pyramidal neurons in the superficial cortex (layer II) were the second most prevalent neuron type observed in the present study. These neurons met the definition of extraversion, with apical dendritic extent exceeding that of the basilar dendritic system (Sanides and Sanides 1972). This neuronal morphology and its laminar distribution are comparable to extraverted pyramidal neurons previously documented in several cetacean species (striped dolphin: Ferrer and Perera 1988; bottlenose dolphin: Glezer et al. 1998; Glezer and Morgane 1990; Morgane et al. 1985; sei whale: Kraus and Pilleri 1969b, c; humpback whale: Hof and Van der Gucht 2007). Extraverted neurons have also been described in terrestrial mammals including bats, hedgehog, opossum and monkeys (Sanides and Sanides 1972), xenarthans and afrotherians (Jacobs et al. 2011; Sherwood et al. 2009), and artiodactyls (Butti et al. 2014; Jacobs et al. 2014a). However, in the current sample, the laminar distribution of these neurons was more restricted than in these other species, where they span layers II, III, and V. In cetaceans, and perhaps in other species (e.g., elephants), these extraverted neurons may facilitate interneuronal communication within superficial cortical layers, where most thalamocortical afferents terminate (Glezer and Morgane 1990).

Magnopyramidal neurons in the present study exhibited a morphology that was essentially identical to that of typical pyramidal neurons, except that the magnopyramidal neurons possessed larger somata and more extensive dendritic arbors. These neurons, which may represent an extreme adaptation of the pyramidal neuron in large brains (Jacobs et al. 2011), have been described in the cetacean literature as “large pyramidal neurons” located in deep cortical layers (bottlenose dolphin: Garey et al. 1985; striped dolphin: Ferrer and Perera 1988; short beaked common dolphin: Kraus and Pilleri 1969a). Magnopyramidal neurons have also been observed in terrestrial species, including the pygmy hippopotamus (Butti et al. 2014), the African elephant (Jacobs et al. 2011), the giraffe (Jacobs et al. 2014a), and primates (de Lima et al. 1990). In

all three species investigated here, magnopyramidal neurons in the visual cortex resembled the solitary cells of Meynert in primates (Hof et al. 2000b; le Gros Clark 1942; Meynert 1867; Winfield and Powell 1983). This finding is consistent with previous reports in the bottlenose dolphin (Furutani 2008) and humpback whale (Hof and Van der Gucht 2007). In the present study, Meynert-like cells in the visual cortex of the humpback whale were especially prominent and evenly spaced ($\sim 500 \mu\text{m}$), a spacing that is slightly greater than the $\sim 400 \mu\text{m}$ noted in giraffes (Jacobs et al. 2014a) and in primates (Chan-Palay et al. 1974; Hof et al. 2000b). Functionally, Meynert cells appear to have evolved to span various cortical layers and to integrate a broad sampling of information (Chan-Palay et al. 1974; Sherwood et al. 2003). It has been suggested that, in primates living in exposed environments, the enlarged Meynert cells represent an anatomical substrate for detecting predators (Sherwood et al. 2003). Although it is tempting to suggest neuromorphological convergent evolution for this trait in cetaceans and primates, the presence of Meynert-like cells in the visual cortex of the bottlenose dolphin may relate to their ability to adjust vision for acuity in air and in water (Herman et al. 1975), although most consider that odontocetes primarily use echolocation rather than vision to navigate their aquatic environment and to locate predators and prey (Au et al. 2009; Au and Nachtigall 1997).

Some of the magnopyramidal neurons in the present investigation approached the soma size and dendritic extent of primate gigantopyramidal neurons, that is, Betz cells in motor cortex (Betz 1881; Braak and Braak 1976). Indeed, there can be overlap in the size of magnopyramidal and gigantopyramidal neurons (Jacobs et al. 2014a; Walshe 1942). In the humpback whale motor cortex, for example, two neurons possessed very large somata, characteristic of Betz cells, along with a thick apical dendrite and many basilar dendrites (Meyer 1987; Scheibel and Scheibel 1978; Sherwood et al. 2003). Betz-like cells were not observed in our Golgi preparations of the bottlenose dolphin and minke whale. This was possibly due to the quality of the impregnation rather than the absence of such neuronal type in these species. Indeed, the somata of magnopyramidal neurons in the motor cortex of the minke whale ($\text{Mean}_{\text{soma size}} = 1,056 \pm 251 \mu\text{m}^2$) are comparable in size to those of gigantopyramidal neurons in the motor cortex of the giraffe ($\text{Mean}_{\text{soma size}} = 1,184 \pm 246 \mu\text{m}^2$; (Jacobs et al. 2014a) and to human Betz cells (Sasaki and Iwata 2001).

Multiapical pyramidal neurons appear to fit somewhere in the middle on a continuum from “typical” to “atypical” pyramidal neurons. Although multiapical pyramidal neurons are morphologically similar to extraverted pyramidal neurons in that they both possess apical bouquets,

multiapical pyramidal neurons also possess well-developed basilar skirts similar to those of typical pyramidal neurons. In addition, multiapical pyramidal neurons tend to be located in deeper cortical layers than are superficial extraverted pyramidal neurons. Multiapical pyramidal neurons comparable to those observed in the present study have been observed in the bottlenose dolphin (Garey et al. 1985) and several other mammals (pygmy hippopotamus: Butti et al. 2014; bat: Ferrer 1987; Ferrer et al. 1986a; rat, mouse, hamster, rabbit, hedgehog: Ferrer et al. 1986a; dog: Ferrer et al. 1986b; African elephant: Jacobs et al. 2011). The morphology observed in the present study (see Fig. 8b: M29; Fig. 9b: H22) particularly resembles the multiapical neurons observed in bats (Ferrer 1987) and the tripolar neurons observed in the rat (Ferrer et al. 1986a; Schwartz and Coleman 1981). Previous studies analyzing axonal course have hypothesized that these neurons could be a source of corticothalamic or contralateral corticocortical projections similar to typical pyramidal neurons but with a more specialized function (Ferrer et al. 1986a).

Bitufted pyramidal neurons. Although there is a lack of agreement on nomenclature concerning bitufted pyramidal neurons in the literature, neurons resembling the “bitufted” neurons in the present study have been observed in several species. Neurons of similar morphology have been labeled “double-bouquet” neurons in striped and bottlenose dolphins (Ferrer and Perera 1988; Glezer et al. 1992; Glezer and Morgane 1990), “vertical fusiform cells” in the macaque monkey (de Lima et al. 1990), “spiny bipolar cells” in the dog (Ferrer et al. 1986b), and “bitufted neurons” in the rock hyrax (Bianchi et al. 2011). It appears that the term “tufted” was applied less stringently in previous studies than in the present one, as the bitufted neurons in the current study possess more dendritically extensive tufts.

Atypical pyramidal neurons

Inverted and horizontal pyramidal neurons. In the present study, inverted pyramidal neurons constituted only a small number of the neurons stained, which is consistent with findings in other species. In the chimpanzee sensorimotor cortex, for example, inverted neurons accounted for <1 % of all pyramidal neurons (Qi et al. 1999). In rats, rabbits, cats, sheep, sloths, anteaters, rock hyrax, and elephant shrews, they constituted 1–8.5 % of all cortical neurons (Mendizabal-Zubiaga et al. 2007; Parnavelas et al. 1977a, b; Sherwood et al. 2009). Functionally, these appear to be excitatory neurons involved in corticocortical, cortico-claustral, and corticostriatal projections in laboratory species (Mendizabal-Zubiaga et al. 2007), providing a

supporting but distinct flow of information to more typical pyramidal neurons (Ferrer et al. 1986a; Mendizabal-Zubiaga et al. 2007).

Horizontal neurons have been described in superficial and deep cortical layers across a wide variety of species including rodents and primates (de Lima et al. 1990; Meyer 1987; Miller 1988), African elephants (Jacobs et al. 2011), cetaceans (bottlenose dolphin: Garey et al. 1985; striped dolphin: Ferrer and Perera 1988), anteaters, sloths, elephant shrews, and rock hyraxes (Bianchi et al. 2011; Sherwood et al. 2009), giraffes (Jacobs et al. 2014a), and lagomorphs, insectivores, and chiropterans (Ferrer et al. 1986a; Mendizabal-Zubiaga et al. 2007). In carnivores, artiodactyls, and primates, there appears to be a different pattern of distribution for horizontal and inverted pyramidal neurons. Horizontal pyramidal neurons are located mainly in intermediate and sulcal parts of cortical gyri whereas inverted pyramidal neurons have been described mainly in the crowns of cortical gyri (Ferrer et al. 1986b). It has consequently been proposed that the “atypical” orientation of inverted and horizontal pyramidal neurons depends on whether they are located in the gyral, intermediate, or sulcal zones (de Lima et al. 1990; Ferrer et al. 1986b), although this fails to explain the presence of these morphologies in both gyrencephalic and lissencephalic mammals (Ferrer et al. 1986a, b).

Flattened pyramidal neurons were also infrequently stained in the current sample. These neurons resemble a neuronal morphology found in the fissural and intermediate cortex of the dog, although these morphologies were classified as “typical” or “horizontal” pyramidal neurons (Ferrer et al. 1986b). Flattened pyramidal neurons have been described in layer VIb of lissencephalic species as neurons with triangular, polygonal or globular somata, apical dendrites that divide into oblique branches shortly after leaving the soma, and a mostly symmetrical array of basilar branches (Ferrer et al. 1986b). More recently, flattened neurons were noted to be abundant in deep layer III and superficial layer V of the African elephant (Jacobs et al. 2011), where they resembled certain cortical neurons in the cow (Barasa 1960), but were generally much more widely bifurcating. The flattened morphology is not widely described in the literature and there is no direct evidence of its function; however, given their horizontal orientation, these neurons may be involved in lateral integration of cortical information, particularly in larger brains (Hart et al. 2008; Jacobs et al. 2011).

Nonpyramidal spiny neurons

Sternzellen were only observed in layers V and VI of the anterior temporal, posterior temporal, and frontal cortices

of the humpback whale. Such results are probably due to the idiosyncrasies of the Golgi impregnation and should not be interpreted as indicating an absence of Sternzellen in the minke whale or bottlenose dolphin. These neurons, originally documented in the sei whale (Kraus and Pilleri 1969c), closely resemble the “spiny stellate” or “spiny multipolar” neurons described in bottlenose and striped dolphins (Ferrer and Perera 1988; Furutani 2008; Garey et al. 1985; Glezer and Morgane 1990). Such neuronal morphology seems to be specific to the cetacean neocortex as there is no definitive evidence of its presence in other species, including artiodactyls (Butler 2008; Butti et al. 2014; Jacobs et al. 2014a). Although the functional significance of this neuronal morphology remains unclear, Sternzellen (or stellate neurons) in agranular mammalian cortices may represent a compensatory mechanism, or evolutionary alternative, to the granularity of most mammalian cortices (Morgane et al. 1985).

Aspiny neurons

Normally, the classification of aspiny neurons is based on axonal morphology (Druga 2009; Lund and Lewis 1993) and is supported by electrophysiological and molecular data (Ascoli et al. 2008; DeFelipe 1997; DeFelipe et al. 2013; Zaitsev et al. 2009). Such classification is sometimes complicated by the fact that many terms for aspiny neurons are also applied to spiny neurons of similar morphologies (Ferrer et al. 1986a, b; Ferrer and Perera 1988; Garey et al. 1985). In the present investigation, only somatodendritic information was available and, as such, the aspiny neurons were classified as either bipolar or multipolar based on their dendritic systems. Bipolar and multipolar aspiny neurons appeared equally represented in the cortical regions across species in the present study, with the exception of the bottlenose dolphin, in which bipolar aspiny neurons were not documented. Bipolar aspiny neurons are found in a variety of mammals under several different labels, such as “bipolar neurons” in the African elephant (Jacobs et al. 2011) and the rock hyrax (Bianchi et al. 2011), “nonspiny spindle neurons” in bottlenose dolphin (Garey et al. 1985), “fusiform neurons” and “bitufted neurons” in rat, dog, sheep, and striped dolphin (Ferrer et al. 1986a, b; Ferrer and Perera 1988; Garey et al. 1985). Multipolar aspiny neurons have been observed in a wide range of species, including striped dolphin (Ferrer and Perera 1988), bottlenose dolphin (Garey et al. 1985), rat, mouse, hamster, bat, dog (Ferrer et al. 1986a, b), African elephant (Jacobs et al. 2011), and rock hyrax (Bianchi et al. 2011).

Although there was considerable variation among the small number of aspiny neurons traced, the humpback whale tended to have the largest aspiny neurons of the three

species. On average, the Vol and TDL of aspiny neurons in the humpback whale are similar to the same measures in the African elephant (Jacobs et al. 2011), but much larger than observed in the giraffe (Jacobs et al. 2014a). Because such quantitative measures are not available for older, qualitative studies, we also examined the dendritic radii of these neurons. Bipolar and multipolar interneurons possessed an average dendritic radius of about 468 and 575 μm in the humpback whale and 300 and 375 μm in the minke whale, respectively. In the bottlenose dolphin, only aspiny multipolar neurons were traced, and these possessed an average radius of 300 μm . By comparison, the dendritic radius of aspiny neurons in the striped dolphin has been documented at 100–300 μm (Ferrer and Perera 1988), and in the African elephant at 1,000 μm . As was the case for Vol and TDL, the dendritic radii in the humpback whale are similar to what has been observed in the elephant.

Comparison of odontocetes and mysticetes

Although generalization about neuronal distributions based on Golgi stains are problematic, we note here that there appeared to be more magnopyramidal neurons in mysticetes than in odontocetes. Nevertheless, previous research has documented magnopyramidal neurons in the bottlenose dolphin visual cortex (Garey et al. 1985). Sternzellen in the present study were observed only in the humpback whale, consistent with a previous description in another mysticete (Kraus and Pilleri 1969a, b, c). Qualitatively, there have been only limited neuromorphological comparisons between odontocetes and mysticetes. For example, possible scaling differences between the sei whale and the short-beaked common dolphin have been suggested because the former possessed neurons with larger somata, longer basilar skirts, and more spines than the latter (Kraus and Pilleri 1969b). Similar conclusions seem reasonable in the present study as dendritic measures (and soma size) increased with brain mass (e.g., bottlenose dolphin < minke whale < humpback whale).

Scaling laws in the brain are very complicated (Deacon 1990), with different orders of mammals having different scaling coefficients (Gabi et al. 2010; Harrison et al. 2002; Herculano-Houzel 2007; Herculano-Houzel et al. 2006, 2007; Neves et al. 2014; Sarko et al. 2009). Most dendritic arbors scale up with brain size, especially in pyramidal neurons (Oelschläger et al. 2010; Wittenberg 2008) and greater neuronal size is found in larger brains (Jacobs et al. 2011; Oelschläger et al. 2010; Wittenberg 2008). In the present study, this was seen quantitatively in typical pyramidal and extraverted pyramidal neurons, which showed increases in dendritic Vol, TDL, and MSL from the bottlenose dolphin to the humpback whale.

Regional cortical differences and specific neuronal morphology in cetaceans

Qualitatively, the variety of neuronal morphologies across cortical regions appeared quite consistent within each species. These results are supported by previous investigations that yielded similar findings between primary auditory and primary visual cortices in striped and bottlenose dolphins (Ferrer and Perera 1988; Glezer et al. 1998). In the current study, the visual cortex represented a unique point of comparison because it was the only cortical area sampled in all three species. Among the variety of spiny neuronal types described in the present study, two morphologies that may be particular to cetaceans were documented: (1) a tri-tufted variant of typical pyramidal and magnopyramidal neurons, and (2) Sternzellen. The tri-tufted variant has not been documented in other mammalian species, suggesting that this neuronal morphology might be a feature present only in cetaceans. Additionally, the presence of Sternzellen in the humpback whale (but not in the minke whale or bottlenose dolphin), coupled with their original description (Kraus and Pilleri 1969b) and the apparent lack of this neuron type in other mammals, suggests that Sternzellen may be a specific characteristic of large baleen whales.

The variety of neuronal morphologies in the cetacean neocortex suggests possible species differences in connectivity and signal integration (Chklovskii 2004; Wen and Chklovskii 2008). For example, comparative analysis of CaBPs has revealed a vertical flow of inhibition in the primary sensory cortices of the bottlenose dolphin, which contrasts with the equal vertical and horizontal flow of inhibition in primates (Glezer et al. 1998). Moreover, layer III in cetaceans appears to have a prevalent role in horizontal integration (Kern et al. 2011). This has interesting implications for the evolution of cortical connectivity. Both the African elephant (Jacobs et al. 2011) and cetaceans possess agranular cortices and, in terms of cytoarchitecture and neuromorphology both appear to possess more lateral cortical communication when compared to other large-brained mammals (Garey et al. 1985; Kern et al. 2011). The presence of extraverted neurons, pyramidal neurons with bifurcating apical dendrites, and laterally oriented neuronal morphologies (e.g., horizontal and flattened pyramidal neurons) suggest a different evolutionary mechanism for intracortical processing in cetaceans. However, it should be noted that pyramidal neurons in cetacean cortex, like those in the giraffe (Jacobs et al. 2014a), appear much more vertically oriented than are pyramidal neurons in the African elephant (Jacobs et al. 2011).

Finally, the present study addresses a controversy in the literature about the nature of the cetacean cortex. Traditionally, certain aspects of cetacean cortical

cytoarchitecture were considered to represent “primitive” features characteristic of a relatively simple cortical organization scheme compared to rodent and primate species (Kesarev et al. 1977; Morgane et al. 1985; Oelschläger and Oelschläger 2008). However, this “initial brain” concept (Glezer et al. 1988) is problematic because cetacean cytoarchitectural patterns are, in fact, more complex than originally thought (Butti et al. 2011; Furutani 2008; Hof et al. 2005; Hof and Van der Gucht 2007; Kern et al. 2011; Marino et al. 2008). The present observations also provide evidence of considerable diversity in neuronal morphology in the cetacean neocortex. Together these findings suggest that these features may actually be derived characters of the cetacean neocortex, rather than plesiomorphic retentions. This is significant, as a previously assumed lack of neuronal variation and neocortical complexity (i.e., agranularity) has been invoked to suggest that cetacean neocortex was underdeveloped (Sokolov et al. 1972; Glezer et al. 1988). Instead, the cetacean neocortex is more comparable to that of other cetartiodactyls (Jacobs et al. 2014a) and perhaps more generally to species lacking layer IV (Ferrer et al. 1986a, b; Ferrer and Perera 1988; Hof et al. 2005; Jacobs et al. 2011). In conclusion, it appears that, in addition to the long-held primate-rodent model of neocortical organization (Manger et al. 2008), other evolutionary alternatives need to be acknowledged and investigated further. To this end, our companion paper and previous studies (Jacobs et al. 2011, 2014a) examine the neuronal morphology of the giraffe, allowing further comparisons within cetartiodactyls and between cetartiodactyls and other species.

Acknowledgments Partial support for this work was provided by Colorado College’s divisional research funds (B.J.), the James S. McDonnell Foundation (Grants 22002078 to C.C.S. and P.R.H., and 220020293 to C.C.S.), and the National Science Foundation (Grants BCS-0515484 and BCS-0824531 to C.C.S.). The authors wish to thank Ms. Kimberly Durham, Mr. Robert DiGiovanni, Ms. Julika N. Wocial, and The Riverhead Foundation for Marine Research and Preservation for precious help during samples collection under MMHSRP’s MMPA/ESA Enhancement and Scientific Research Permit NMFS Permit No. 932-1905/MA-009526, and the National Marine Fisheries Service (NOAA Fisheries) for permission to collect samples from stranded specimens to Dr. Joy Reidenberg.

References

- Anderson K, Bones B, Robinson B, Hass C, Lee H, Ford K, Roberts TA, Jacobs B (2009) The morphology of supragranular pyramidal neurons in the human insular cortex: a quantitative Golgi study. *Cereb Cortex* 19:2131–2144
- Ascoli GA, Alonso-Nanclares L, Anderson SA, Barrionuevo G, Benavides-Piccione R, Burkhalter A, Buzsaki G, Cauli B, Defelipe J, Fairen A, Feldmeyer D, Fishell G, Fregnac Y, Freund TF, Gardner D, Gardner EP, Goldberg JH, Helmstaedter M, Hestrin S, Karube F, Kisvarday ZF, Lambolez B, Lewis DA,

- Marin O, Markram H, Munoz A, Packer A, Petersen CC, Rockland KS, Rossier J, Rudy B, Somogyi P, Staiger JF, Tamas G, Thomson AM, Toledo-Rodriguez M, Wang Y, West DC, Yuste R (2008) Petilla terminology: nomenclature of features of GABAergic interneurons of the cerebral cortex. *Nat Rev Neurosci* 9:557–568
- Au WW, Nachtigall PE (1997) Acoustics of echolocating dolphins and small whales. *Mar Freshw Behav Physiol* 29:127–162
- Au WW, Branstetter BK, Benoit-Bird KJ, Kastelein RA (2009) Acoustic basis for fish prey discrimination by echolocating dolphins and porpoises. *J Acoust Soc Am* 126:460
- Barasa A (1960) Form, size and density of the neurons in the cerebral cortex of mammals of different body sizes. *Z Zellforsch Mikrosk Anat* 53:69–89
- Betz W (1881) Ueber die feinere Struktur der Gehirnrinde des Menschen. *Zentralbl Med Wiss* 19:193–195
- Bianchi S, Bauernfeind AL, Gupta K, Stimpson CD, Spocter MA, Bonar CJ, Manger PR, Hof PR, Jacobs B, Sherwood CC (2011) Neocortical neuron morphology in Afrotheria: comparing the rock hyrax with the African elephant. *Ann N Y Acad Sci* 1225:37–46
- Bok S (1959) Histonomy of the cerebral cortex. *Histonomy of the cerebral cortex*, Amsterdam
- Boothe RG, Greenough WT, Lund JS, Wrege K (1979) A quantitative investigation of spine and dendrite development of neurons in visual cortex (area17) of *Macaca nemestrina* monkeys. *J Comp Neurol* 186:473–489
- Bota M, Swanson LW (2007) The neuron classification problem. *Brain Res Rev* 56:79–88
- Braak H, Braak E (1976) The pyramidal cells of Betz within the cingulate and precentral gigantopyramidal field in the human brain: a Golgi and pigmentarchitectonic study. *Cell Tissue Res* 172:103–119
- Buell S (1982) Golgi–Cox and rapid Golgi methods as applied to autopsied human brain tissue: widely disparate results. *J Neuro-pathol Exp Neurol* 41:500–507
- Butler AB (2008) Evolution of brains, cognition, and consciousness. *Brain Res Bull* 75:442–449
- Butti C, Hof PR (2010) The insular cortex: a comparative perspective. *Brain Struct Funct* 214:477–493
- Butti C, Sherwood CC, Hakeem AY, Allman JM, Hof PR (2009) Total number and volume of von Economo neurons in the cerebral cortex of cetaceans. *J Comp Neurol* 515:243–259
- Butti C, Raghanti MA, Sherwood CC, Hof PR (2011) The neocortex of cetaceans: cytoarchitecture and comparison with other aquatic and terrestrial species. *Ann N Y Acad Sci* 1225:47–58
- Butti C, Ewan Fordyce R, Ann Raghanti M, Gu X, Bonar CJ, Wicinski BA, Wong EW, Roman J, Brake A, Eaves E, Spocter MA, Tang CY, Jacobs B, Sherwood CC, Hof PR (2014) The cerebral cortex of the pygmy hippopotamus, *Hexaprotodon liberiensis* (Cetartiodactyla, Hippopotamidae): MRI, cytoarchitecture, and neuronal morphology. *Anat Rec* 297:670–700
- Chan-Palay V, Palay SL, Billings-Gagliardi SM (1974) Meynert cells in the primate visual cortex. *J Neurocytol* 3:631–658
- Chklovskii DB (2004) Synaptic connectivity and neuronal morphology: two sides of the same coin. *Neuron* 43:609–617
- Connor RC (2007) Dolphin social intelligence: complex alliance relationships in bottlenose dolphins and a consideration of selective environments for extreme brain size evolution in mammals. *Philos Trans R Soc Lond B Biol Sci* 362:587–602
- Cupp CJ, Uemura E (1980) Age-related changes in the prefrontal cortex of *Macaca mulatta*: quantitative analysis of dendritic branching patterns. *Exp Neurol* 69:143–163
- de Lima AD, Voigt T, Morrison JH (1990) Morphology of the cells within the inferior temporal gyrus that project to the prefrontal cortex in the macaque monkey. *J Comp Neurol* 296:159–172
- de Ruiter JP (1983) The influence of post-mortem fixation delay on the reliability of the Golgi silver impregnation. *Brain Res* 266:143–147
- Deacon TW (1990) Rethinking mammalian brain evolution. *Am Zool* 30:629–705
- DeFelipe J (1997) Types of neurons, synaptic connections and chemical characteristics of cells immunoreactive for calbindin-D28K, parvalbumin and calretinin in the neocortex. *J Chem Neuroanat* 14:1–19
- DeFelipe J, Lopez-Cruz PL, Benavides-Piccione R, Bielza C, Larranaga P, Anderson S, Burkhalter A, Cauli B, Fairen A, Feldmeyer D, Fishell G, Fitzpatrick D, Freund TF, Gonzalez-Burgos G, Hestrin S, Hill S, Hof PR, Huang J, Jones EG, Kawaguchi Y, Kisvarday Z, Kubota Y, Lewis DA, Marin O, Markram H, McBain CJ, Meyer HS, Monyer H, Nelson SB, Rockland K, Rossier J, Rubenstein JL, Rudy B, Scanziani M, Shepherd GM, Sherwood CC, Staiger JF, Tamas G, Thomson A, Wang Y, Yuste R, Ascoli GA (2013) New insights into the classification and nomenclature of cortical GABAergic interneurons. *Nat Rev Neurosci* 14:202–216
- Druga R (2009) Neocortical inhibitory system. *Folia Biol* 55:201–217
- Elias H, Schwartz D (1969) Surface areas of the cerebral cortex of mammals determined by stereological methods. *Science* 166:111–113
- Elston GN, Rosa MG (1998a) Complex dendritic fields of pyramidal cells in the frontal eye field of the macaque monkey: comparison with parietal areas 7a and LIP. *NeuroReport* 9:127–131
- Elston GN, Rosa MG (1998b) Morphological variation of layer III pyramidal neurones in the occipitotemporal pathway of the macaque monkey visual cortex. *Cereb Cortex* 8:278–294
- Elston GN, Oga T, Fujita I (2009) Spinogenesis and pruning scales across functional hierarchies. *J Neurosci* 29:3271–3275
- Elston GN, Oga T, Okamoto T, Fujita I (2010a) Spinogenesis and pruning from early visual onset to adulthood: an intracellular injection study of layer III pyramidal cells in the ventral visual cortical pathway of the macaque monkey. *Cereb Cortex* 20:1398–1408
- Elston GN, Okamoto T, Oga T, Dornan D, Fujita I (2010b) Spinogenesis and pruning in the primary auditory cortex of the macaque monkey (*Macaca fascicularis*): an intracellular injection study of layer III pyramidal cells. *Brain Res* 1316:35–42
- Elston GN, Oga T, Okamoto T, Fujita I (2011) Spinogenesis and pruning in the anterior ventral inferiotemporal cortex of the macaque monkey: an intracellular injection study of layer III pyramidal cells. *Front Neuroanat* 5:42
- Eriksen N, Pakkenberg B (2007) Total neocortical cell number in the mysticete brain. *Anat Rec* 290:83–95
- Ferrer I (1987) The basic structure of the neocortex in insectivorous bats (*Miniopterus shreibersi* and *Pipistrellus pipistrellus*). A Golgi study. *J Hirnforsch* 28:237–243
- Ferrer I, Perera M (1988) Structure and nerve cell organisation in the cerebral cortex of the dolphin *Stenella coeruleoalba* a Golgi study. With special attention to the primary auditory area. *Anat Embryol* 178:161–173
- Ferrer I, Fábregues I, Condom E (1986a) A Golgi study of the sixth layer of the cerebral cortex. I. The lissencephalic brain of Rodentia, Lagomorpha, Insectivora and Chiroptera. *J Anat* 145:217–234
- Ferrer I, Fábregues I, Condom E (1986b) A Golgi study of the sixth layer of the cerebral cortex. II. The gyrencephalic brain of Carnivora, Artiodactyla and Primates. *J Anat* 146:87–104
- Furutani R (2008) Laminar and cytoarchitectonic features of the cerebral cortex in the Risso's dolphin (*Grampus griseus*), striped dolphin (*Stenella coeruleoalba*), and bottlenose dolphin (*Tursiops truncatus*). *J Anat* 213:241–248

- Gabi M, Collins CE, Wong P, Torres LB, Kaas JH, Herculano-Houzel S (2010) Cellular scaling rules for the brains of an extended number of primate species. *Brain Behav Evol* 76:32–44
- Garey LJ, Winkelmann E, Brauer K (1985) Golgi and Nissl studies of the visual cortex of the bottlenose dolphin. *J Comp Neurol* 240:305–321
- Garey LJ, Takacs J, Revishchin AV, Hamori J (1989) Quantitative distribution of GABA-immunoreactive neurons in cetacean visual cortex is similar to that in land mammals. *Brain Res* 485:278–284
- Garland EC, Noad MJ, Goldizen AW, Lilley MS, Rekdahl ML, Garrigue C, Constantine R, Daeschler Hauser N, Poole MM, Robbins J (2013) Quantifying humpback whale song sequences to understand the dynamics of song exchange at the ocean basin scale. *J Acoust Soc Am* 133:560–569
- Gatesy J (1997) More DNA support for a Cetacea/Hippopotamidae clade: the blood-clotting protein gene gamma-fibrinogen. *Mol Biol Evol* 14:537–543
- Geisler G, Uhen MD (2003) Morphological support for a close relationship between hippos and whales. *J Vert Paleontol* 23:991–996
- Germroth P, Schwerdtfeger WK, Buhl EH (1989) Morphology of identified entorhinal neurons projecting to the hippocampus. A light microscopical study combining retrograde tracing and intracellular injection. *Neuroscience* 30:683–691
- Gingerich PD, Uhen MD (1998) Likelihood estimation of the time of origin of cetacean and the time of divergence of Cetacea and Artiodactyla. *Paleo-Electronica* 2:1–47
- Gingerich PD, Haq M, Zalmout IS, Khan IH, Malkani MS (2001) Origin of whales from early artiodactyls: hands and feet of Eocene Protocetidae from Pakistan. *Science* 293:2239–2242
- Glezer I (2002) Neural morphology. In: Hoesel AR (ed) *Marine mammal biology: an evolutionary approach*. Blackwell Science Ltd, Malden, pp 98–115
- Glezer II, Morgane PJ (1990) Ultrastructure of synapses and Golgi analysis of neurons in neocortex of the lateral gyrus (visual cortex) of the dolphin and pilot whale. *Brain Res Bull* 24:401–427
- Glezer II, Jacobs MS, Morgane PJ (1988) Implications of the “initial brain” concept for brain evolution in Cetacea. *Behav Brain Sci* 11:75–116
- Glezer II, Hof PR, Morgane PJ (1992) Calretinin-immunoreactive neurons in the primary visual cortex of dolphin and human brains. *Brain Res* 595:181–188
- Glezer II, Hof PR, Leraneth C, Morgane PJ (1993) Calcium-binding protein-containing neuronal populations in mammalian visual cortex: a comparative study in whales, insectivores, bats, rodents, and primates. *Cereb Cortex* 3:249–272
- Glezer I, Hof PR, Morgane PJ (1995) Cytoarchitectonics and immunocytochemistry of the inferior colliculus of midbrain in cetaceans. *FASEB J* 9:A247
- Glezer II, Hof PR, Morgane PJ (1998) Comparative analysis of calcium-binding protein-immunoreactive neuronal populations in the auditory and visual systems of the bottlenose dolphin (*Tursiops truncatus*) and the macaque monkey (*Macaca fascicularis*). *J Chem Neuroanat* 15:203–237
- Hanson A, Grisham W, Sheh C, Annese J, Ridgway S (2013) Quantitative examination of the bottlenose dolphin cerebellum. *Anat Rec* 296:1215–1228
- Harrison KH, Hof PR, Wang SS (2002) Scaling laws in the mammalian neocortex: does form provide clues to function? *J Neurocytol* 31:289–298
- Hart BL, Hart LA, Pinter-Wollman N (2008) Large brains and cognition: where do elephants fit in? *Neurosci Biobehav Rev* 32:86–98
- Hassiotis M, Ashwell KW (2003) Neuronal classes in the isocortex of a monotreme, the Australian echidna (*Tachyglossus aculeatus*). *Brain Behav Evol* 61:6–27
- Herculano-Houzel S (2007) Encephalization, neuronal excess, and neuronal index in rodents. *Anat Rec* 290:1280–1287
- Herculano-Houzel S, Mota B, Lent R (2006) Cellular scaling rules for rodent brains. *Proc Natl Acad Sci USA* 103:12138–12143
- Herculano-Houzel S, Collins CE, Wong P, Kaas JH (2007) Cellular scaling rules for primate brains. *Proc Natl Acad Sci USA* 104:3562–3567
- Herman LM, Tavolga WN (1980) The communication systems of cetaceans. In: Herman LM (ed) *Cetacean behavior: mechanisms and functions*. Wiley, New York, pp 149–209
- Herman LM, Peacock MF, Yunker MP, Madsen CJ (1975) Bottlenosed dolphin: double-slit pupil yields equivalent aerial and underwater diurnal acuity. *Science* 189:650–652
- Hof PR, Sherwood CC (2005) Morphomolecular neuronal phenotypes in the neocortex reflect phylogenetic relationships among certain mammalian orders. *Anat Rec* 287:1153–1163
- Hof PR, Van der Gucht E (2007) Structure of the cerebral cortex of the humpback whale, *Megaptera novaeangliae* (Cetacea, Mysticeti, Balaenopteridae). *Anat Rec* 290:1–31
- Hof PR, Glezer II, Archin N, Janssen WG, Morgane PJ, Morrison JH (1992) The primary auditory cortex in cetacean and human brain: a comparative analysis of neurofilament protein-containing pyramidal neurons. *Neurosci Lett* 146:91–95
- Hof PR, Glezer II, Revishchin AV, Bouras C, Charnay Y, Morgane PJ (1995) Distribution of dopaminergic fibers and neurons in visual and auditory cortices of the harbor porpoise and pilot whale. *Brain Res Bull* 36:275–284
- Hof PR, Glezer II, Condé F, Flagg RA, Rubin MB, Nimchinsky EA, Vogt Weisenhorn DM (1999) Cellular distribution of the calcium-binding proteins parvalbumin, calbindin, and calretinin in the neocortex of mammals: phylogenetic and developmental patterns. *J Chem Neuroanat* 16:77–116
- Hof PR, Glezer II, Nimchinsky EA, Erwin JM (2000a) Neurochemical and cellular specializations in the mammalian neocortex reflect phylogenetic relationships: evidence from primates, cetaceans, and artiodactyls. *Brain Behav Evol* 55:300–310
- Hof PR, Nimchinsky EA, Young WG, Morrison JH (2000b) Numbers of Meynert and layer IVB cells in area V1: a stereologic analysis in young and aged macaque monkeys. *J Comp Neurol* 420:113–126
- Hof PR, Chanis R, Marino L (2005) Cortical complexity in cetacean brains. *Anat Rec* 287:1142–1152
- Huggenberger S (2008) The size and complexity of dolphin brains—A paradox? *J Mar Biol Assoc UK* 88:1103–1108
- Jacobs B, Scheibel AB (1993) A quantitative dendritic analysis of Wernicke’s area in humans. I. Lifespan changes. *J Comp Neurol* 327:83–96
- Jacobs B, Scheibel AB (2002) Regional dendritic variation in primate cortical pyramidal cells. In: Schuz A, Miller R (eds) *Cortical areas: unity and diversity (Conceptual advances in brain research series)*. Taylor & Francis, London, pp 111–131
- Jacobs MS, Morgane PJ, McFarland WL (1971) The anatomy of the brain of the bottlenose dolphin (*Tursiops truncatus*). Rhinencephalon. I. The paleocortex. *J Comp Neurol* 141:205–271
- Jacobs MS, McFarland WL, Morgane PJ (1979) The anatomy of the brain of the bottlenose dolphin (*Tursiops truncatus*). Rhinencephalon: the archicortex. *Brain Res Bull* 1:1–108
- Jacobs MS, Galaburda AM, McFarland WL, Morgane PJ (1984) The insular formations of the dolphin brain: quantitative cytoarchitectonic studies of the insular component of the limbic lobe. *J Comp Neurol* 225:396–432

- Jacobs B, Driscoll L, Schall M (1997) Lifespan dendritic and spine changes in areas 10 and 18 of human cortex: a quantitative Golgi study. *J Comp Neurol* 386:661–680
- Jacobs B, Schall M, Prather M, Kapler E, Driscoll L, Baca S, Jacobs J, Ford K, Wainwright M, Trembl M (2001) Regional dendritic and spine variation in human cerebral cortex: a quantitative Golgi study. *Cereb Cortex* 11:558–571
- Jacobs B, Lubs J, Hannan M, Anderson K, Butti C, Sherwood CC, Hof PR, Manger PR (2011) Neuronal morphology in the African elephant (*Loxodonta africana*) neocortex. *Brain Struct Funct* 215:273–298
- Jacobs B, Harland T, Kennedy D, Schall M, Wicinski B, Butti C, Hof PR, Sherwood CC, Manger PR (2014a) The neocortex of cetartiodactyls. II. Neuronal morphology of the visual and motor cortices in the giraffe (*Giraffa camelopardalis*). *Brain Struct Funct*. doi:10.1007/s00429-014-0830-9
- Jacobs B, Johnson NL, Wahl D, Schall M, Maseko BC, Lewandowski A, Raghanti MA, Wicinski B, Butti C, Hopkins WD, Bertelsen MF, Walsh T, Roberts JR, Reep RL, Hof PR, Sherwood CC, Manger PR (2014b) Comparative neuronal morphology of the cerebellar cortex in afrotherians, carnivores, cetartiodactyls, and primates. *Front Neuroanat* 8:24
- Kawaguchi Y (1995) Physiological subgroups of nonpyramidal cells with specific morphological characteristics in layer II/III of rat frontal cortex. *J Neurosci* 15:2638–2655
- Kern A, Siebert U, Cozzi B, Hof PR, Oelschläger HH (2011) Stereology of the neocortex in odontocetes: qualitative, quantitative, and functional implications. *Brain Behav Evol* 77:79–90
- Kesarev VS (1971) The inferior brain of the dolphin. *Soviet Sci Rev* 2:52–58
- Kesarev VS (1975) Homologization of the cerebral neocortex in cetaceans. *Arkhiv Anat Gistol Embriol* 68:5–13
- Kesarev VS, Malofeeva LI (1969) Structural organization of the motor zone of the cerebral cortex in dolphins. *Arkh Anat Gistol Embriol* 56:48–55
- Kesarev VS, Malofeeva LI, Trykova OV (1977) Structural organization of the cetacean neocortex. *Arkh Anat Gistol Embriol* 73:23–30
- Kisvarday ZF, Gulyas A, Beroukas D, North JB, Chubb IW, Somogyi P (1990) Synapses, axonal and dendritic patterns of GABA-immunoreactive neurons in human cerebral cortex. *Brain* 113:793–812
- Kraus C, Pilleri G (1969a) Quantitative Untersuchungen über die Grosshirnrinde der Cetaceen. *Investig Cetacea* 1:127–150
- Kraus C, Pilleri G (1969b) Zur Feinstruktur der großen Pyramidenzellen in der V Cortexschicht der Cetacean (*Delphinus delphis* und *Balaenoptera borealis*). *Investig Cetacea* 1:89–99
- Kraus C, Pilleri G (1969c) Zur Histologie der Grosshirnrinde von *Balaenoptera borealis* Lesson (Cetacea, Mysticeti). *Investig Cetacea* 1:151–170
- Ladygina TF, Supin A (1977) Localization of the sensory projection areas in the cerebral cortex of the dolphin, *Tursiops truncatus*. *Zh Evol Biokhim Fiziol* 13:712–718
- Ladygina TF, Mass AM, Supin A (1978) Multiple sensory projections in the dolphin cerebral cortex. *Zh Vyssh Nerv Deiat Pavl* 28:1047–1053
- Le Gros Clark WE (1942) The cells of Meynert in the visual cortex of the monkey. *J Anat* 76:369–376
- Lopez-Mascaraque L, De Carlos JA, Valverde F (1986) Structure of the olfactory bulb of the hedgehog (*Erinaceus europaeus*): description of cell types in the granular layer. *J Comp Neurol* 253:135–152
- Lund JS, Lewis DA (1993) Local circuit neurons of developing and mature macaque prefrontal cortex: Golgi and immunocytochemical characteristics. *J Comp Neurol* 328:282–312
- Manger PR (2006) An examination of cetacean brain structure with a novel hypothesis correlating thermogenesis to the evolution of a big brain. *Biol Rev Camb Philos Soc* 81:293–338
- Manger PR (2013) Questioning the interpretations of behavioral observations of cetaceans: is there really support for a special intellectual status for this mammalian order? *Neuroscience* 250:664–696
- Manger P, Sum M, Szymanski M, Ridgway SH, Krubitzer L (1998) Modular subdivisions of dolphin insular cortex: does evolutionary history repeat itself? *J Cogn Neurosci* 10:153–166
- Manger PR, Fuxe K, Ridgway SH, Siegel JM (2004) The distribution and morphological characteristics of catecholaminergic cells in the diencephalon and midbrain of the bottlenose dolphin (*Tursiops truncatus*). *Brain Behav Evol* 64:42–60
- Manger PR, Cort J, Ebrahim N, Goodman A, Henning J, Karolia M, Rodrigues SL, Strkalj G (2008) Is 21st century neuroscience too focussed on the rat/mouse model of brain function and dysfunction? *Front Neuroanat* 2:5
- Manger PR, Prowse M, Haagensen M, Hemingway J (2012) Quantitative analysis of neocortical gyrencephaly in African elephants (*Loxodonta africana*) and six species of cetaceans: comparison with other mammals. *J Comp Neurol* 520:2430–2439
- Marino L (2002) Convergence of complex cognitive abilities in cetaceans and primates. *Brain Behav Evol* 59:21–32
- Marino L, Murphy TL, Deweerd AL, Morris JA, Fobbs AJ, Humblot N, Ridgway SH, Johnson JI (2001a) Anatomy and three-dimensional reconstructions of the brain of the white whale (*Delphinapterus leucas*) from magnetic resonance images. *Anat Rec* 262:429–439
- Marino L, Murphy TL, Gozal L, Johnson JI (2001b) Magnetic resonance imaging and three-dimensional reconstructions of the brain of a fetal common dolphin, *Delphinus delphis*. *Anat Embryol* 203:393–402
- Marino L, Sudheimer KD, Murphy TL, Davis KK, Pabst DA, McLellan WA, Rilling JK, Johnson JI (2001c) Anatomy and three-dimensional reconstructions of the brain of a bottlenose dolphin (*Tursiops truncatus*) from magnetic resonance images. *Anat Rec* 264:397–414
- Marino L, Sudheimer KD, Pabst DA, McLellan WA, Filsoof D, Johnson JI (2002) Neuroanatomy of the common dolphin (*Delphinus delphis*) as revealed by magnetic resonance imaging (MRI). *Anat Rec* 268:411–429
- Marino L, Sudheimer K, Pabst DA, McLellan WA, Johnson JI (2003a) Magnetic resonance images of the brain of a dwarf sperm whale (*Kogia simus*). *J Anat* 203:57–76
- Marino L, Sudheimer K, Sarko D, Sirpenski G, Johnson JI (2003b) Neuroanatomy of the harbor porpoise (*Phocoena phocoena*) from magnetic resonance images. *J Morphol* 257:308–347
- Marino L, Sherwood CC, Delman BN, Tang CY, Naidich TP, Hof PR (2004a) Neuroanatomy of the killer whale (*Orcinus orca*) from magnetic resonance images. *Anat Rec* 281:1256–1263
- Marino L, Sudheimer K, McLellan WA, Johnson JI (2004b) Neuroanatomical structure of the spinner dolphin (*Stenella longirostris orientalis*) brain from magnetic resonance images. *Anat Rec* 279:601–610
- Marino L, Connor RC, Fordyce RE, Herman LM, Hof PR, Lefebvre L, Lusseau D, McCowan B, Nimchinsky EA, Pack AA, Rendell L, Reidenberg JS, Reiss D, Uhen MD, Van der Gucht E, Whitehead H (2007) Cetaceans have complex brains for complex cognition. *PLoS Biol* 5:e139
- Marino L, Butti C, Connor RC, Fordyce RE, Herman LM, Hof PR, Lefebvre L, Lusseau D, McCowan B, Nimchinsky EA, Pack AA, Reidenberg JS, Reiss D, Rendell L, Uhen MD, Van der Gucht E, Whitehead H (2008) A claim in search of evidence: reply to

- Manger's thermogenesis hypothesis of cetacean brain structure. *Biol Rev Camb Philos Soc* 83:417–440
- Masland RH (2004) Neuronal cell types. *Curr Biol* 14:R497–R500
- Mendizabal-Zubiaga JL, Reblet C, Bueno-Lopez JL (2007) The underside of the cerebral cortex: layer V/VI spiny inverted neurons. *J Anat* 211:223–236
- Meyer G (1987) Forms and spatial arrangement of neurons in the primary motor cortex of man. *J Comp Neurol* 262:402–428
- Meynert T (1867) Der Bau der Grosshirnrinde und seine örtlichen Verschiedenheiten nebst einem pathologisch anatomischen Corollarium. *Vierteljahrsch Psychiatr* 198–217
- Milinkovitch M, Bérubé M, Palsboll PJ (1998) Cetaceans are highly derived artiodactyls. In: Thewissen JGM (ed) *The emergence of whales*. Plenum Press, New York, pp 113–131
- Miller MW (1988) Maturation of rat visual cortex: IV. The generation, migration, morphogenesis, and connectivity of atypically oriented pyramidal neurons. *J Comp Neurol* 274:387–405
- Montie EW, Schneider GE, Ketten DR, Marino L, Touhey KE, Hahn ME (2007) Neuroanatomy of the subadult and fetal brain of the Atlantic white-sided dolphin (*Lagenorhynchus acutus*) from in situ magnetic resonance images. *Anat Rec* 290:1459–1479
- Montie EW, Schneider G, Ketten DR, Marino L, Touhey KE, Hahn ME (2008) Volumetric neuroimaging of the Atlantic white-sided dolphin (*Lagenorhynchus acutus*) brain from in situ magnetic resonance images. *Anat Rec* 291:263–282
- Morgane P, Jacobs M, McFarland W (1980) The anatomy of the brain of the bottlenose dolphin (*Tursiops truncatus*). Surface configuration of the telencephalon of the bottlenose dolphin with comparative anatomical observations in four other Cetaceans species. *Brain Res Bull* 5:1–107
- Morgane PJ, McFarland WL, Jacobs MS (1982) The limbic lobe of the dolphin brain: a quantitative cytoarchitectonic study. *J Hirnforsch* 23:465–552
- Morgane PJ, Jacobs MS, Galaburda A (1985) Conservative features of neocortical evolution in dolphin brain. *Brain Behav Evol* 26:176–184
- Morgane PJ, Glezer II, Jacobs MS (1988) Visual cortex of the dolphin: an image analysis study. *J Comp Neurol* 273:3–25
- Morgane P, Glezer I, Jacobs M (1990) Comparative and evolutionary anatomy of the visual cortex of the dolphin. In: Jones EG, Peters A (eds) *Cerebral cortex. Comparative structure and evolution of cerebral cortex, part II, vol 8B*. Plenum Press, New York, pp 215–262
- Neves K, Ferreira FM, Tovar-Moll F, Gravett N, Bennett NC, Kaswera C, Gilissen E, Manger PR, Herculano-Houzel S (2014) Cellular scaling rules for the brain of afrotherians. *Front Neuroanat* 8:5
- Nikaido M, Rooney AP, Okada N (1999) Phylogenetic relationships among cetartiodactyls based on insertions of short and long interspersed elements: hippopotamuses are the closest extant relatives of whales. *Proc Natl Acad Sci USA* 96:10261–10266
- Nikaido M, Matsuno F, Hamilton H, Brownell RL Jr, Cao Y, Ding W, Zuoyan Z, Shedlock AM, Fordyce RE, Hasegawa M, Okada N (2001) Retroposon analysis of major cetacean lineages: the monophyly of toothed whales and the paraphyly of river dolphins. *Proc Natl Acad Sci USA* 98:7384–7389
- Oelschläger HA, Oelschläger JS (2008) Brain. In: Perrin WF, Würsig B, Thewissen JGM (eds) *Encyclopedia of marine mammals*. Academic Press, San Diego, pp 134–149
- Oelschläger HH, Haas-Rioth M, Fung C, Ridgway SH, Knauth M (2008) Morphology and evolutionary biology of the dolphin (*Delphinus* sp.) brain—MR imaging and conventional histology. *Brain Behav Evol* 71:68–86
- Oelschläger HH, Ridgway SH, Knauth M (2010) Cetacean brain evolution: dwarf sperm whale (*Kogia sima*) and common dolphin (*Delphinus delphis*)—an investigation with high-resolution 3D MRI. *Brain Behav Evol* 75:33–62
- Parnavelas JG, Lieberman AR, Webster KE (1977a) Organization of neurons in the visual cortex, area 17, of the rat. *J Anat* 124:305–322
- Parnavelas JG, Sullivan K, Lieberman AR, Webster KE (1977b) Neurons and their synaptic organization in the visual cortex of the rat. *Electron microscopy of Golgi preparations*. *Cell Tissue Res* 183:499–517
- Patzke N, Spocter MA, Karlsson KA, Bertelsen MF, Haagensen M, Chawana R, Streicher S, Kaswera C, Gilissen E, Alagaili AN, Mohammed OB, Reep RL, Bennett NC, Siegel JM, Ihunwo AO, Manger PR (2013) In contrast to many other mammals, cetaceans have relatively small hippocampi that appear to lack adult neurogenesis. *Brain Struct Funct*. doi:10.1007/s00429-013-0660-1
- Peters A, Jones EG (1984) Classification of cortical neurons. In: Peters A, Jones EG (eds) *Cerebral cortex: cellular components of the cerebral cortex, vol 1*. Plenum Press, New York, pp 107–121
- Peters A, Regidor J (1981) A reassessment of the forms of nonpyramidal neurons in area 17 of cat visual cortex. *J Comp Neurol* 203:685–716
- Qi HX, Jain N, Preuss TM, Kaas JH (1999) Inverted pyramidal neurons in chimpanzee sensorimotor cortex are revealed by immunostaining with monoclonal antibody SMI-32. *Somatosens Mot Res* 16:49–56
- Revishchin AV, Garey LJ (1989) Sources of thalamic afferent neurons, projecting into the suprasylvian gyrus of the dolphin cerebral cortex. *Neirofiziol* 21:529–539
- Ridgway S, Brownson RH (1984) Relative brain sizes and cortical surface areas in odontocetes. *Acta Zool Fenn* 172:149–152
- Sanides F, Sanides D (1972) The “extraverted neurons” of the mammalian cerebral cortex. *Z Anat Entwickl-gesch* 136:272–293
- Sarko DK, Catania KC, Leitch DB, Kaas JH, Herculano-Houzel S (2009) Cellular scaling rules of insectivore brains. *Front Neuroanat* 3:8
- Sasaki S, Iwata M (2001) Ultrastructural study of Betz cells in the primary motor cortex of the human brain. *J Anat* 199:699–708
- Scheibel ME, Scheibel AB (1978) The methods of Golgi. In: *Neuroanatomical research techniques*. Academic Press, New York, pp 89–114
- Schwartz SP, Coleman PD (1981) Neurons of origin of the perforant path. *Exp Neurol* 74:305–312
- Sherwood CC, Lee PW, Rivara CB, Holloway RL, Gilissen EP, Simmons RM, Hakeem A, Allman JM, Erwin JM, Hof PR (2003) Evolution of specialized pyramidal neurons in primate visual and motor cortex. *Brain Behav Evol* 61:28–44
- Sherwood CC, Stimpson CD, Butti C, Bonar CJ, Newton AL, Allman JM, Hof PR (2009) Neocortical neuron types in Xenarthra and Afrotheria: implications for brain evolution in mammals. *Brain Struct Funct* 213:301–328
- Shimamura M, Yasue H, Ohshima K, Abe H, Kato H, Kishiro T, Goto M, Munechika I, Okada N (1997) Molecular evidence from retroposons that whales form a clade within even-toed ungulates. *Nature* 388:666–670
- Shimamura M, Abe H, Nikaido M, Ohshima K, Okada N (1999) Genealogy of families of SINEs in cetaceans and artiodactyls: the presence of a huge superfamily of tRNA(Glu)-derived families of SINEs. *Mol Biol Evol* 16:1046–1060
- Sholl DA (1953) Dendritic organization in the neurons of the visual and motor cortices of the cat. *J Anat* 87:387–406
- Sokolov VE, Ladygina TF, Supin A (1972) Localization of sensory zones in the dolphin cerebral cortex. *Proc Acad Sci USSR* 202:490–493

- Somogyi P, Kisvarday ZF, Martin KA, Whitteridge D (1983) Synaptic connections of morphologically identified and physiologically characterized large basket cells in the striate cortex of cat. *Neuroscience* 10:261–294
- Thewissen JG, Williams EM, Roe LJ, Hussain ST (2001) Skeletons of terrestrial cetaceans and the relationship of whales to artiodactyls. *Nature* 413:277–281
- Thewissen JGM, Cooper LN, Clementz MT, Bajpai S, Tiwari BN (2007) Whales originated from aquatic artiodactyls in the Eocene epoch of India. *Nature* 450:1190–1194
- Travis K, Ford K, Jacobs B (2005) Regional dendritic variation in neonatal human cortex: a quantitative Golgi study. *Dev Neurosci* 27:277–287
- Uylings HB, Ruiz-Marcos A, van Pelt J (1986) The metric analysis of three-dimensional dendritic tree patterns: a methodological review. *J Neurosci Methods* 18:127–151
- Walshe F (1942) The giant cells of Betz, the motor cortex and the pyramidal tract: a critical review. *Brain* 65:409–461
- Wen Q, Chklovskii DB (2008) A cost–benefit analysis of neuronal morphology. *J Neurophysiol* 99:2320–2328
- Williams RS, Ferrante RJ, Caviness VS Jr (1978) The Golgi rapid method in clinical neuropathology: the morphologic consequences of suboptimal fixation. *J Neuropathol Exp Neurol* 37:13–33
- Winfield DA, Powell TP (1983) Laminar cell counts and geniculocortical boutons in area 17 of cat and monkey. *Brain Res* 277:223–229
- Wittenberg GMWS (2008) Evolution and scaling of dendrites. In: Stuart G, Spruston N, Häusser M (eds) *Dendrites*. Oxford University Press, New York, pp 43–67
- Zaitsev AV, Povysheva NV, Gonzalez-Burgos G, Rotaru D, Fish KN, Krimer LS, Lewis DA (2009) Interneuron diversity in layers 2–3 of monkey prefrontal cortex. *Cereb Cortex* 19:1597–1615